Organometallics 1993, *12*, 2714–2725

Reactivity of the Lewis Acids $Cp^*M(NO)(CH_2CMe_3)Cl$ [M = Mo, W] and Related Complexes

Jeff D. Debad, Peter Legzdins,* Steven J. Rettig, and John E. Veltheer

Department of Chemistry, The University of British Columbia,
Vancouver, British Columbia, Canada V6T 1Z1

Received February 18, 1993

Treatments of $Cp^*M(NO)Cl_2$ [$Cp^* = \eta^5\text{-}C_5Me_5$; M = Mo, W] with 0.5 equiv of $(Me_3CCH_2)_2Mg\cdot X(\text{dioxane})$ in THF at low temperatures affords the monoalkylated complexes, $Cp^*M(NO)(CH_2CMe_3)Cl$ (**1**, **1′**). Exposure to a second 0.5 equiv of $(Me_3CCH_2)_2Mg\cdot X(\text{dioxane})$ at higher temperatures produces the dialkyl complexes, $Cp^*M(NO)(CH_2CMe_3)_2$ (**2**, **2′**). Utilizing the two series of $Cp^*M(NO)Cl_2$, $Cp^*M(NO)(CH_2CMe_3)Cl$ and $Cp^*M(NO)(CH_2CMe_3)_2$ complexes, the relative electron deficiencies in these 16-electron complexes can be assessed spectroscopically and electrochemically. Without exception, the Mo complexes are the stronger Lewis acids. Also, the mononeopentyl derivatives for both metals are more reactive toward a variety of substrates than are their bis(neopentyl) analogues. Complexes **1** and **1′** serve as precursors to mixed alkyl and alkyl aryl complexes (**3**, **3′**, **4**, **4′**) and yield metal-centered adducts with PMe_3 and pyridine (**5**, **5′**, **6**, **6′**). CO and $CNCMe_3$ readily insert into the M–C bonds of **1** and **1′**. The insertion products, $Cp^*M(NO)(C\{E\}CH_2CMe_3)Cl$ (**7**, **7′**, E = O; **8**, **8′**, E = $NCMe_3$), have η^2-acyl and -iminoacyl ligands, the former being confirmed by the solid-state structural analysis of $Cp^*Mo(NO)(\eta^2\text{-}C\{O\}CH_2CMe_3)Cl$ (**7**). Crystal data for **7**: $a = 15.226(2)$ Å, $b = 12.376(2)$ Å, $c = 19.641(2)$ Å, $\beta = 95.921(8)°$, $Z = 8$, space group $P2_1/n$, $R_F = 0.032$, $R_{wF} = 0.032$ for 7215 reflections with $I \geq 3\sigma(I)$. The chloride ligands in $Cp^*M(NO)(CH_2CMe_3)Cl$ are easily abstracted by Ag^+ in NCMe to form alkyl cations of the type $[Cp^*M(NO)(CH_2CMe_3)(NCMe)_x]BF_4$ (**9**, $x = 1$; **9′**, $x = 2$). The acyl complex, $Cp^*W(NO)(\eta^2\text{-}C\{O\}CH_2CMe_3)Cl$, reacts with PMe_3 to form the metal-centered η^1-acyl adduct (**10′**). The other phosphine complexes, $Cp^*M(NO)(CH_2CMe_3)(Cl)(PMe_3)$, are readily dehydrohalogenated by lithium diisopropylamide in THF to afford cyclometalated complexes of the type $(\eta^5,\eta^1\text{-}C_5Me_4CH_2)M(NO)(CH_2CMe_3)(PMe_3)$ (**11**, **11′**). The solid state structure of the W species (**11′**) has been established. Crystal data for **11′**: $a = 14.323(1)$ Å, $b = 16.861(2)$ Å, $c = 8.511(2)$ Å, $Z = 4$, space group $P2_12_12_1$, $R_F = 0.030$, $R_{wF} = 0.024$ for 2420 reflections with $I \geq 3\sigma(I)$. The structures of **7** and **11′** were solved by conventional heavy atom methods and were refined by full-matrix least-squares procedures.

Introduction

Interest continues to be directed toward transition-metal complexes that contain metal–carbon σ bonds, especially those with coordinatively and/or electronically unsaturated metal centers. This fact is due not only to the synthetic utility of such complexes because of their involvement in a variety of stoichiometric and catalytic transformations,[1] but is also a reflection of the desire of many researchers to continue elucidating the fascinating fundamental chemistry of transition-metal-carbon bonds.[2] The chemistry of complexes containing unsaturated metal centers is often dominated by the Lewis acidity of the compound. For instance, the catalytic activity of the lanthanide and actinide complexes, Cp^*_2ScR [R = alkyl, H][3] and $Cp^*_2M(R)X$ [M = Th, U, X = halide, alkoxide][4] is ascribed to their highly Lewis acidic metal centers. Fine tuning of coordinative unsaturation can also be accomplished by variation of hydrocarbyl, ancillary or cyclopentadienyl ligand steric and electronic requirements.[5]

Our recent efforts in this area have centered principally on the characteristic stoichiometric chemistry of hydrocarbon ligands attached to the 14-valence-electron fragments, $Cp'M(NO)$ [M = Mo or W; $Cp' = Cp(\eta^5\text{-}C_5H_5)$ or $Cp^*(\eta^5\text{-}C_5Me_5)$]. In particular, we initially expended considerable effort in developing the chemistry of the symmetric 16-electron complexes, $Cp'M(NO)R_2$ [R = alkyl, aryl].[6] Subsequently, we developed methodology to synthesize asymmetric tungsten complexes of the type $Cp'W(NO)(R)R'$[7] and were thus afforded the opportunity to study the comparative reactivity of two different hydrocarbyl ligands attached to the same metal center.[8] In general, the preparation of asymmetric hydrocarbyl complexes, $L_nM(R)R'$, has not been trivial and has presented significant synthetic challenges. This state of affairs is often attributed to the difficulty in preparing the requisite precursor complexes, $L_nM(R)X$ [X = halide].[9] In this paper, we report the results of our investigations of the fundamental chemical properties of two prototypal alkyl chloro complexes, $Cp^*M(NO)(CH_2CMe_3)Cl$ [M =

---

(1) Collman, J. P.; Hegedus, L. S.; Norton, J. R.; Finke, R. G. *Principles and Applications of Organotransition Metal Chemistry*; University Science Books: Mill Valley, CA, 1987; Chapters 3 and 14.

(2) *The Chemistry of the Metal-Carbon Bond*; Hartley, F. R., Patai, S., Eds.; Wiley: New York, 1985; Vol 2.

(3) Piers, W. E.; Shapiro, P. J.; Bunel, E. E.; Bercaw, J. E. *Synlett* **1990**, 74 and refs therein.

(4) Lin, Z.; Marks, T. J. *J. Am. Chem. Soc.* **1987**, *109*, 7979 and refs therein.

(5) Our own efforts in this area are summarized in ref 6. An excellent study by Marks and co-workers on linked-Cp_2MR [M = Lu, Y] complexes can be found in Stern, D.; Sabat, M.; Marks, T. J. *J. Am. Chem. Soc.* **1990**, *112*, 9558 and refs therein.

(6) Legzdins, P.; Veltheer, J. E. *Acc. Chem. Res.* **1993**, *26*, 41.

(7) Debad, J. D.; Legzdins, P.; Batchelor, R. J.; Einstein, F. W. B. *Organometallics* **1992**, *11*, 6.

(8) Debad, J. D.; Legzdins, P.; Batchelor, R. J.; Einstein, F. W. B. *Organometallics*, in press.

0276-7333/93/2312-2714$04.00/0

Table I. Numbering Scheme, Color, Isolated Yield, and Elemental Analysis Data for Complexes 1–11 and 1′–11′

complex	compd no.	color (yield, %)	anal. found (calcd) C	H	N
$Cp^*Mo(NO)(CH_2CMe_3)Cl$	1	violet (55)	48.97 (48.99)	7.05 (7.13)	3.88 (3.81)
$Cp^*W(NO)(CH_2CMe_3)Cl$	1′	purple (63)	39.25 (39.54)	5.80 (5.75)	2.89 (3.07)
$Cp^*Mo(NO)(CH_2CMe_3)_2$	2	red (59)	59.70 (59.54)	9.35 (9.24)	3.50 (3.47)
$Cp^*W(NO)(CH_2CMe_3)_2$	2′	red (31)	48.60 (48.89)	7.63 (7.59)	2.89 (2.85)
$Cp^*Mo(NO)(CH_2CMe_3)(CH_2SiMe_3)$	3	red (41)	54.35 (54.40)	8.91 (8.89)	3.25 (3.34)
$Cp^*W(NO)(CH_2CMe_3)(CH_2CMe_2Ph)$	3′	maroon (40)	54.28 (54.25)	7.13 (7.10)	2.42 (2.53)
$Cp^*Mo(NO)(CH_2CMe_3)(p\text{-tolyl})$	4	maroon (30)	62.38 (62.40)	7.80 (7.85)	3.50 (3.31)
$Cp^*W(NO)(CH_2CMe_3)(p\text{-tolyl})$	4′	purple (49)	51.72 (51.67)	6.52 (6.50)	2.63 (2.74)
$Cp^*Mo(NO)(CH_2CMe_3)(PMe_3)Cl$	5	yellow (49)	48.89 (48.71)	7.79 (7.95)	3.25 (3.16)
$Cp^*W(NO)(CH_2CMe_3)(PMe_3)Cl$	5′	orange (78)	40.91 (40.66)	6.83 (6.63)	2.56 (2.63)
$Cp^*Mo(NO)(CH_2CMe_3)(py)Cl$	6	orange (86)	53.88 (53.76)	7.06 (6.99)	6.48 (6.27)
$Cp^*W(NO)(CH_2CMe_3)(py)Cl$	6′	orange (53)	44.82 (44.92)	5.92 (5.84)	5.24 (5.24)
$Cp^*Mo(NO)(\eta^2\text{-}C\{O\}CH_2CMe_3)Cl$	7	amber (30)	48.63 (48.56)	6.56 (6.62)	3.43 (3.54)
$Cp^*W(NO)(\eta^2\text{-}C\{O\}CH_2CMe_3)Cl$	7′	yellow (71)	39.91 (39.73)	5.60 (5.42)	2.86 (2.90)
$Cp^*Mo(NO)(\eta^2\text{-}C\{NCMe_3\}CH_2CMe_3)Cl$	8	yellow (95)	53.47 (53.28)	7.80 (7.82)	6.27 (6.21)
$Cp^*W(NO)(\eta^2\text{-}C\{NCMe_3\}CH_2CMe_3)Cl$	8′	yellow (85)	44.41 (44.58)	6.44 (6.55)	5.10 (5.20)
$[Cp^*Mo(NO)(CH_2CMe_3)(NCMe)]BF_4$	9	yellow (86)	43.58 (44.37)	6.27 (6.35)	5.57 (6.09)
$[Cp^*W(NO)(CH_2CMe_3)(NCMe)_2]BF_4$	9′	orange (66)	38.56 (38.73)	5.59 (5.48)	7.09 (7.13)
$Cp^*W(NO)(\eta^1\text{-}C\{O\}CH_2CMe_3)(PMe_3)Cl$	10′	orange (76)	40.86 (40.76)	6.37 (6.30)	2.46 (2.50)
$(\eta^5,\eta^1\text{-}C_5Me_4CH_2)Mo(NO)(CH_2CMe_3)(PMe_3)$	11	amber (64)	53.04 (53.07)	8.51 (8.41)	3.37 (3.44)
$(\eta^5,\eta^1\text{-}C_5Me_4CH_2)W(NO)(CH_2CMe_3)(PMe_3)$	11′	orange (46)	43.33 (43.65)	6.90 (6.92)	2.79 (2.83)

Mo, W], which are the precursors to bis(hydrocarbyl) compounds. Specifically, we describe their straightforward synthesis, their characterization and reactivity. Finally, we contrast the chemical properties of these compounds, particularly their abilities to function as Lewis acids, with those exhibited by their symmetrical analogues, $Cp^*M(NO)(CH_2CMe_3)_2$ and $Cp^*M(NO)Cl_2$.

Experimental Section

All reactions and subsequent manipulations were performed under anaerobic and anhydrous conditions using an atmosphere of prepurified argon. General procedures, including electrochemical techniques, routinely employed in our laboratories have been described in detail previously.[10] The compounds $Cp^*M(NO)Cl_2$,[11] $Cp^*W(NO)(CH_2CMe_3)Cl$ (1′),[8] $(Me_3SiCH_2)_2Mg\cdot X(dioxane)$,[12] $(Me_3CCH_2)_2Mg\cdot X(dioxane)$,[12] $(PhMe_2CCH_2)_2Mg\cdot X(dioxane)$,[12] $(p\text{-tolyl})_2Mg\cdot X(dioxane)$,[10] and PMe_3[13] were prepared by their published procedures. Other reagents such as CO (Matheson), $CNCMe_3$, $AgBF_4$, and LDA ($LiN(i\text{-}Pr)_2$) (Aldrich) were used as received. Pyridine and acetonitrile (BDH) were twice distilled from CaH_2.

Isolated yields and elemental analysis data for all product complexes are listed in Table I, while their spectroscopic and physical properties are collected in Tables I–III.

Preparation of $Cp^*Mo(NO)(CH_2CMe_3)Cl$ (1). $Cp^*Mo(NO)Cl_2$ (332 mg, 1.00 mmol) and $(Me_3CCH_2)_2Mg\cdot X(dioxane)$ (0.50 mmol) were weighed into a Schlenk tube. THF (40 mL) was then vacuum-transferred onto the solids at −196 °C. The stirred reaction mixture was allowed to warm slowly to −45 °C whereupon the insoluble orange $Cp^*Mo(NO)Cl_2$ slowly dissolved into the increasingly purple solution (ν_{NO} 1618 cm^{-1}). When no solid $Cp^*Mo(NO)Cl_2$ remained in the bottom of the Schlenk tube, the reaction was deemed to be complete (2–6 h). The reaction mixture was then warmed to −10 °C, and the THF was removed in vacuo. The oily purple residue was suspended in pentane (25 mL), stirred for 15 min at room temperature, and then taken to dryness to obtain a purple powder. The powder was extracted with pentane/Et_2O (4:1, 3 × 30 mL). The combined extracts were filtered through Celite (2 × 5 cm) supported on a glass frit and then concentrated in vacuo. Maintaining this solution at −30 °C for several days induced the precipitation of purple needles of 1 which were collected by filtration. Upon drying in vacuo the needles became a purple powder.

For preparative purposes, solutions of $Cp^*Mo(NO)(CH_2CMe_3)Cl$ (ca. 90% yield)[14] were used directly after the Celite filtration described in the preceding paragraph.

Preparation of $Cp^*Mo(NO)(CH_2CMe_3)_2$ (2). $Cp^*Mo(NO)Cl_2$ (332 mg, 1.00 mmol) and $(Me_3CCH_2)_2Mg\cdot X(dioxane)$ (1.00 mmol) were weighed into a Schlenk tube. THF (15 mL) was vacuum-transferred onto the solids at −196 °C. The stirred reaction mixture was slowly allowed to warm to 0 °C whereupon the solution first turned purple then red (ν_{NO} 1588 cm^{-1}). The red solution was taken to dryness in vacuo. The residue was suspended in Et_2O (30 mL), treated with 2 drops of water, and quickly transferred onto a column of neutral alumina I (2 × 3 cm) supported on a glass frit. The column was washed with Et_2O (30 mL) until the eluate was colorless. The ether was then removed from the eluate to obtain a red powder which was dissolved in a minimum of pentane (5 mL) and crystallized at −30 °C overnight. Large red crystals of 2 were isolated by removing the mother liquor via cannulation.

Preparation of $Cp^*W(NO)(CH_2CMe_3)_2$ (2′). $Cp^*W(NO)(CH_2CMe_3)Cl$ (150 mg, 0.330 mmol) and $(Me_3CCH_2)_2Mg\cdot X(dioxane)$ (0.165 mmol) were weighed into a Schlenk tube. THF (20 mL) was vacuum-transferred onto the combined solids at −196 °C. The stirred reaction mixture was warmed to room temperature. The resulting brown-red solution (ν_{NO} 1568 cm^{-1}) was taken to dryness and extracted with pentane (2 × 10 mL). The red pentane solution was filtered through Celite (2 × 3 cm) supported on a glass frit. The filtrate was concentrated and placed in a freezer (−30 °C) to induce crystallization. After 4 d, red crystals of 2′ were isolated by removing the mother liquor via cannulation.

---

(9) Selected examples of successfully prepared halo hydrocarbyl complexes are $Cp_2Zr(Me)Cl$,[9a,b] $Cp^*Ru(NO)(Ph)Cl$,[9c] $(Me_3P)_4Ru(Me)Cl$,[9d] $(PNP)Ir(Me)I$ [PNP = $N(SiMe_2CH_2PPh_2)_2$],[9e] $Cp^*_2Th(CH_2SiMe_3)Cl$,[9f] and $(\eta^5\text{-indenyl})Ir(PMe)_3(R)I$ [R = Ph, *p*-tolyl, Me].[9g] (a) Carr, D. B.; Schwartz, J. *J. Am. Chem. Soc.* **1979**, *101*, 3521. (b) Gell, K. I.; Posin, B.; Schwartz, J.; Williams, G. M. *J. Am. Chem. Soc.* **1982**, *104*, 1846 and refs therein. (c) Chang, J.; Seidler, M. D.; Bergman, R. G. *J. Am. Chem. Soc.* **1989**, *111*, 3258. (d) Hartwig, J. F.; Andersen, R. A.; Bergman, R. G. *J. Am. Chem. Soc.* **1989**, *111*, 2717. (e) Fryzuk, M. D.; MacNeil, P. A.; Rettig, S. J. *J. Am. Chem. Soc.* **1985**, *107*, 6708. (f) Bruno, J. W.; Smith, G. M.; Marks, T. J.; Fair, C. K.; Schultz, A. J.; Williams, J. M. *J. Am. Chem. Soc.* **1986**, *108*, 40. (g) Foo, T.; Bergman, R. G. *Organometallics* **1992**, *11*, 1801.

(10) Dryden, N. H.; Legzdins, P.; Rettig, S. J.; Veltheer, J. E. *Organometallics* **1992**, *11*, 2583.

(11) Dryden, N. H.; Legzdins, P.; Batchelor, R. J.; Einstein, F. W. B. *Organometallics* **1991**, *10*, 2077.

(12) Dryden, N. H.; Legzdins, P.; Trotter, J.; Yee, V. C. *Organometallics* **1991**, *10*, 2857.

(13) Wolfsberger, W.; Schmidbaur, H. *Synth. React. Inorg. Met.-Org. Chem.* **1974**, *4*, 149.

(14) Several reactions of this type were taken to dryness in tared flasks, and the weight of the crude product was established by difference. The yields of four separate experiments ranged from 83–93%.

Table II. Mass Spectral and Infrared Data for Complexes 1–11 and 1′–11′

compd no.	MS m/z^a	temp^b (°C)	IR (Nujol mull)	
			ν_{NO}	other bands
1	*c*	–	1606 (vs)	–
1′	455 [P^+]	100	1582 (vs)	–
2	405 [P^+]	150	1593 (vs)	1235 (w, CMe_3)
2′	491 [P^+]	80	1557 (vs)	1285 (w, CMe_3)
3	421 [P^+]	100	1599 (vs)	–
3′	553 [P^+]	180	1570 (vs)	–
4	425 [P^+]	150	1611 (vs)	–
4′	511 [P^+]	120	1555 (vs)	–
5	387 [$P^+ - CH_2CMe_3$], 369 [$P^+ - PMe_3$]	DCI^d	1575 (vs)	1233 (w, CMe_3), 958 (m, PMe_3)
5′	455 [$P^+ - PMe_3$]	180	1553 (vs)	1285 (w, CMe_3)
6	*c*	–	1600 (sh), 1580 (s), 1561 (s)	1223 (w, CMe_3)
6′	455 [$P^+ - NC_5H_5$]	120	1549 (vs)	–
7	397 [P^+]	180	1624 (vs)	1246 (w, CMe_3), 1601 (s, CO)
7′	483 [P^+], 455 [$P^+ - CO$]	180	1584 (vs)	1564 (s, CO)
8	452 [P^+], 422 [$P^+ - NO$]	180	1574 (vs)	1715 (m, CN), 1231 (w, CMe_3)
8′	538 [P^+], 508 [$P^+ - NO$]	200	1537 (vs)	1680 (m, CN)
9	462 [P^+]	+FAB^e	1606 (vs)	2316, 2290 (NCMe), 1230 (w, CMe_3), 1063 (br, BF_4)
9′	589 [P^+]	+FAB^e	1589 (vs)	2319, 2291 (NCMe), 1060 (br, BF_4)
10′	483 [$P^+ - PMe_3$]	180	1580 (vs)	1634 (s, CO)
11	409 [P^+]	120	1595 (m), 1544 (br)	952 (m, PMe_3)
11′	495 [P^+]	180	1524 (vs)	953 (m, PMe_3)

[a] m/z values are for the highest intensity peak of the calculated isotopic cluster, i.e. ^{98}Mo and ^{184}W. [b] Probe temperatures. [c] Decomposes. [d] NH_3 carrier. [e] FAB-MS (matrix: 3-nitrobenzyl alcohol).

Preparation of $Cp^*Mo(NO)(CH_2CMe_3)(CH_2SiMe_3)$ (3). $Cp^*Mo(NO)(CH_2CMe_3)Cl$ (262 mg, 0.71 mmol) and $(Me_3SiCH_2)_2Mg\cdot X$(dioxane) (0.35 mmol) were weighed into a Schlenk tube. Et_2O (25 mL) was vacuum-transferred onto the solids at −196 °C. The stirred reaction mixture was slowly allowed to warm to 0 °C whereupon the burgundy reaction mixture was taken to dryness in vacuo. The residue was extracted with pentane (2 × 10 mL), and the combined extracts were filtered through a pad of Celite (2 × 2 cm). The filtrate was taken to dryness in vacuo to provide **3** as an analytically pure red powder.

Preparation of $Cp^*W(NO)(CH_2CMe_3)(CH_2CMe_2Ph)$ (3′). $Cp^*W(NO)Cl_2$ (840 mg, 2.00 mmol) and $(Me_3CCH_2)_2Mg\cdot X$(dioxane) (1.00 mmol) were weighed into a Schlenk tube. THF (20 mL) was vacuum-transferred onto the solids at −196 °C. The stirred reaction mixture was warmed to room temperature, whereupon the THF was removed in vacuo, and the remaining purple residue was dried in vacuo for 1 h. The residue was then suspended in Et_2O (30 mL) and cooled to −30 °C. A solution of $(PhMe_2CCH_2)_2Mg\cdot X$(dioxane) (0.97 mmol) in Et_2O (10 mL) was slowly cannulated into the Et_2O suspension of $Cp^*W(NO)(CH_2CMe_3)Cl$. The resulting mixture was warmed to room temperature and filtered through a Florisil column (2 × 2 cm) supported on a glass frit. The column was rinsed with Et_2O (30 mL) until the eluate was colorless. The solvent was removed from the red eluate, and the residue was dried in vacuo for several hours before being redissolved in a minimum of pentane. This pentane solution of **3′** was cooled overnight at −30 °C, whereupon maroon crystals formed. The mother liquor was separated from the crystals by cannulation and was further concentrated and cooled to −30 °C overnight to obtain a second crop of crystals of **3′**.

Preparation of $Cp^*M(NO)(CH_2CMe_3)$(*p*-tolyl) (4 and 4′). These complexes were prepared in a manner similar to that described for **3** and **3′** (vide supra) except that (*p*-tolyl)$_2Mg\cdot X$(dioxane) was used in the second alkylation step. The complexes were crystallized from Et_2O.

Preparation of $Cp^*Mo(NO)(CH_2CMe_3)(PMe_3)Cl$ (5). A solution of $Cp^*Mo(NO)(CH_2CMe_3)Cl$ (0.90 mmol) in Et_2O (10 mL) was treated with excess PMe_3 which was vacuum-transferred from Na/benzophenone. The purple solution became orange immediately. The orange solution was concentrated slightly and cooled for 1 week in a freezer (−30 °C) to obtain large yellow blocks of **5**.

Preparation of $Cp^*W(NO)(CH_2CMe_3)(PMe_3)Cl$ (5′). Into a purple solution of $Cp^*W(NO)(CH_2CMe_3)Cl$ (75 mg, 0.165 mmol) in pentane (10 mL) was vacuum-transferred an excess of PMe_3. The mixture became yellow immediately, and a yellow precipitate formed. The reaction mixture was taken to dryness in vacuo, and the residue was then redissolved in a minimum of Et_2O. Slow cooling of the ether solution to −30 °C yielded orange prisms of **5′**. The crystals were isolated by removing the mother liquor via cannulation. A second fraction of **5′** was obtained by additional concentration and cooling of the mother liquor.

Preparation of $Cp^*M(NO)(CH_2CMe_3)(py)Cl$ (6 and 6′). Violet solutions of $Cp^*M(NO)(CH_2CMe_3)Cl$ (0.50 mmol) in Et_2O (10 mL) were treated with an excess of pyridine (0.50 mL) at room temperature with no change in color being evident. Upon cooling to −30 °C, the reaction solutions became orange-red and the desired product complexes crystallized. **6** and **6′** were isolated as orange crystals which were dried in vacuo at −30 °C. Prolonged drying at room temperature caused the complexes to lose pyridine and darken to red-purple, the characteristic color of their $Cp^*M(NO)(CH_2CMe_3)Cl$ precursors.

Preparation of $Cp^*Mo(NO)(\eta^2\text{-}C\{O\}CH_2CMe_3)Cl$ (7). A sample of $Cp^*Mo(NO)(CH_2CMe_3)Cl$ (188 mg, 0.511 mmol) contained in a 300-mL heavy-walled reaction vessel was dissolved in Et_2O (25 mL). The solution was frozen at −196 °C and thoroughly degassed via several freeze-pump-thaw cycles. The vessel was charged with CO (2 atm) and then warmed to room temperature. The reaction solution changed from purple to brown over the course of 4 h after which time the CO and solvent were removed in vacuo. The brown residue was extracted with hexanes/Et_2O (1:2, 85 mL), and the extracts were filtered through Celite (2 × 2 cm) supported on a glass frit. The filtrate was then concentrated and cooled to −30 °C to induce crystallization. Amber needles of **7** were isolated by removal of the mother liquor by cannulation.

Preparation of $Cp^*W(NO)(\eta^2\text{-}C\{O\}CH_2CMe_3)Cl$ (7′). A sample of $Cp^*W(NO)(CH_2CMe_3)Cl$ (100 mg, 0.220 mmol) was dissolved in pentane (10 mL), and an atmosphere of CO was then introduced into the flask. Over the course of 2 h, a yellow precipitate formed. The supernate was then removed by cannulation, and the precipitate was dissolved in a minimum of Et_2O (20 mL). Keeping the Et_2O solution in a freezer (−30 °C) for several days induced the precipitation of a yellow microcrystalline solid which was isolated by removing the mother liquor with a pipette.

Preparation of $Cp^*M(NO)(\eta^2\text{-}C\{NCMe_3\}CH_2CMe_3)Cl$ (8 and 8′). Samples of $Cp^*M(NO)(CH_2CMe_3)Cl$ (0.500 mmol) contained in a 100-mL reaction vessel were dissolved in Et_2O (10 mL) and taken into a drybox. To the solutions were added aliquots of $CNCMe_3$ (~100 μL, ~0.9 mmol) via a pipette. The solutions instantly changed from purple to amber, and within

Table III. NMR Data for Complexes 1–11 and 1′–11′ (C_6D_6)

compd no.	^1H NMR, δ	$^{13}C\{^1H\}$ NMR, δ
1	3.73 (d, 1H, CH_2, J_{HH} = 10.8 Hz), 1.44 (s, 15H, Cp*), 1.24 (s, 9 H, $C(CH_3)_3$), –0.06 (d, 1H, CH_2, J_{HH} = 10.8 Hz)	113.69 (CH_2), 110.41 ($C_5(CH_3)_5$), 40.12 ($C(CH_3)_3$), 32.89 ($C(CH_3)_3$), 9.86 ($C_5(CH_3)_5$)
1′	3.42 (d, 1H, CH_2, J_{HH} = 12.0 Hz), 1.61 (s, 15H, Cp*), 1.37 (s, 9H, $C(CH_3)_3$), –0.03 (d, 1H, CH_2, J_{HH} = 12.0 Hz)	112.63 ($C_5(CH_3)_5$), 96.59 (CH_2), 39.02 ($C(CH_3)_3$), 33.72 ($C(CH_3)_3$), 9.75 ($C_5(CH_3)_5$)
1^a	3.68 (d, 1H, CH_2, J_{HH} = 11.1 Hz), 1.87 (s, 15H, Cp*), 1.15 (s, 9H, $C(CH_3)_3$), 0.11 (d, 1H, CH_2, J_{HH} = 11.1 Hz)	*b*
1′^{a}	2.92 (d, 1H, CH_2, J_{HH} = 11.1 Hz), 1.89 (s, 15H, Cp*), 1.13 (s, 9H, $C(CH_3)_3$), –0.02 (d, 1H, CH_2, J_{HH} = 11.1 Hz)	*b*
2	3.08 (d, 2H, CH_2, J_{HH} = 12.1 Hz), 1.61 (s, 18H, $C(CH_3)_3$), 1.45 (s, 15H, Cp*), –0.95 (d, 2H, CH_2, J_{HH} = 12.1 Hz)	109.78 ($C_5(CH_3)_5$), 97.97 (CH_2), 39.05 ($C(CH_3)_3$), 33.85 ($C(CH_3)_3$), 9.92 ($C_5(CH_3)_5$)
2′	2.73 (d, 2H, CH_2, J_{HH} = 12.0 Hz), 1.51 (s, 15H, Cp*), 1.34 (s, 18H, $C(CH_3)_3$), –1.42 (d, 2H, CH_2, J_{HH} = 12.0 Hz)	109.57 ($C_5(CH_3)_5$), 95.25 (CH_2), 38.97 ($C(CH_3)_3$), 34.47 ($C(CH_3)_3$), 9.83 ($C_5(CH_3)_5$)
3	3.96 (d, 1H, CH_2CMe_3, $^2J_{HH}$ = 10.8 Hz), 1.51 (s, 15H, Cp*), 1.33 (s, 9H, $CH_2C(CH_3)_3$), 1.19 (d, 1H, CH_2SiMe_3, $^2J_{HH}$ = 12.0 Hz, $^2J_{SiH}$ = 19.8 Hz), 0.37 (s, 9H, $CH_2Si(CH_3)_3$), –0.67 (d, 1H, CH_2SiMe_3, $^2J_{HH}$ = 12.0 Hz, $^4J_{HH}$ = 1.8 Hz), –2.15 (d, 1H, CH_2CMe_3, $^2J_{HH}$ = 10.8 Hz, $^4J_{HH}$ = 1.8 Hz)	118.78 (CH_2CMe_3), 110.06 ($C_5(CH_3)_5$), 46.21 (CH_2SiMe_3), 40.86 ($C(CH_3)_3$), 33.43 ($C(CH_3)_3$), 9.96 ($C_5(CH_3)_5$), 2.57 ($Si(CH_3)_3$)
3′	7.51 (d, 2H, H_{ortho}, J_{HH} = 8.4 Hz), 7.22 (t, 2H, H_{meta}, J_{HH} = 7.8 Hz), 7.06 (t, 1H, H_{para}, J_{HH} = 7.8 Hz), 2.96 (d, 1H, CH_2, $^2J_{HH}$ = 12.6 Hz), 2.72 (d, 1H, CH_2, $^2J_{HH}$ = 13.2 Hz), 1.84 (s, 3H, $C(CH_3)_2Ph$), 1.75 (s, 3H, $C(CH_3)_2Ph$), 1.44 (s, 15H, Cp*), 1.27 (s, 9H, $C(CH_3)_3$), 0.77 (dd, 1H, CH_2, $^2J_{HH}$ = 13.2 Hz, $^4J_{HH}$ = 3.0 Hz), –1.92 (dd, 1H, CH_2, $^2J_{HH}$ = 12.6 Hz, $^4J_{HH}$ = 3.0 Hz)	153.61 (C_{ipso}), 128.41 (C_{ortho}), 126.30 (C_{meta}), 125.45 (C_{para}), 109.70 ($C_5(CH_3)_5$), 102.01 (CH_2, J_{CW} = 92.4 Hz), 92.58 (CH_2, J_{CW} = 96.6 Hz), 45.41 ($C(CH_3)_3$), 39.63 ($C(CH_3)_2Ph$), 34.22 ($C(CH_3)_3$), 34.05 ($C(CH_3)_2Ph$), 32.65 ($C(CH_3)_2Ph$), 9.68 ($C_5(CH_3)_5$)
4	7.71 (d, 2H, H_{ortho}, J_{HH} = 7.8 Hz), 7.14 (d, 2H, H_{meta}, J_{HH} = 7.8 Hz), 4.67 (d, 1H, CH_2, $^2J_{HH}$ = 9.0 Hz), 2.22 (s, 3H, *p*-CH_3), 1.57 (s, 15H, Cp*), 1.28 (s, 9H, $C(CH_3)_3$), –1.55 (d, 1H, CH_2, $^2J_{HH}$ = 9.0 Hz)	*b*
4′	7.68 (d, 2H, H_{ortho}, J_{HH} = 7.2 Hz), 7.03 (d, 2H, H_{meta}, J_{HH} = 7.2 Hz), 4.03 (d, 1H, CH_2, $^2J_{HH}$ = 11.7 Hz), 2.09 (s, 3H, *p*-CH_3), 1.59 (s, 15H, Cp*), 1.25 (s, 9H, $C(CH_3)_3$), –1.87 (d, 1H, CH_2, $^2J_{HH}$ = 11.7 Hz)	179.91 (C_{ipso}), 137.29 (C_{para}), 137.21 (C_{ortho}), 128.69 (C_{meta}), 118.50 (CH_2), 110.82 ($C_5(CH_3)_5$), 40.80 ($C(CH_3)_3$), 34.02 ($C(CH_3)_3$), 21.76 (*p*-CH_3), 10.08 ($C_5(CH_3)_5$)
5^c	2.30 (dd, 1H, CH transoidal to P, J_{HH} = 9.6 Hz, J_{HP} = 3.3 Hz), 1.79 (s, 9H, $C(CH_3)_3$), 1.69 (s, 15H, Cp*), 1.53 (d, 1H, CH cisoidal to P, J_{HH} = 9.6 Hz), 1.32 (d, 9H, $P(CH_3)_3$, J_{HP} = 9.6 Hz)	109.79 ($C_5(CH_3)_5$), 64.70 (d, CH_2, J_{CP} = 7.3 Hz), 38.50 ($C(CH_3)_3$), 35.16 ($C(CH_3)_3$), 12.42 (d, $P(CH_3)_3$, J_{CP} = 26.6 Hz), 9.75 ($C_5(CH_3)_5$)
5′^{c}	1.83 (s, 15H, Cp*), 1.49 (d, 9H, $P(CH_3)_3$, J_{HP} = 9.9 Hz), 1.26 (dd, 1H, CH transoidal to P, J_{HH} = 11.4 Hz, J_{HP} = 4.2 Hz), 1.04 (s, 9H, $C(CH_3)_3$), 0.915 (d, 1H, CH cisoidal to P, J_{HH} = 11.4 Hz)	109.03 ($C_5(CH_3)_5$), 61.70 (d, CH_2, J_{CP} = 9.8 Hz), 37.59 ($C(CH_3)_3$), 34.92 ($C(CH_3)_3$), 12.03 (d, $P(CH_3)_3$, J_{CP} = 30.1 Hz), 9.97 ($C_5(CH_3)_5$)
6^d	8.98 (br s, 2H, py), 8.04 (br s, 1H, py), 7.61 (br s, 2H, py), 2.08 (br s, 1H, CH_2), 1.53 (br s, 15H, Cp*), 1.10 (br s, 9H, $C(CH_3)_3$), 0.49 (br s, 1H, CH_2)	*b*
6′^{d}	9.02 (br s, 2H, py), 8.07 (br s, 1H, py), 7.62 (br s, 2H, py), 2.03 (br s, 1H, CH_2), 1.59 (br s, 15H, Cp*), 1.09 (br s, 9H, $C(CH_3)_3$), 0.26 (br s, 1H, CH_2)	*b*
7	3.08 (d, 1H, CH_2, J_{HH} = 15.5 Hz), 2.62 (d, 1H, CH_2, J_{HH} = 15.5 Hz), 1.61 (s, 15H, Cp*), 0.91 (s, 9H, $C(CH_3)_3$)	280.66 (CO), 112.97 ($C_5(CH_3)_5$), 54.34 (CH_2), 33.08 ($C(CH_3)_3$), 29.64 ($C(CH_3)_3$), 10.10 ($C_5(CH_3)_5$)
7′	3.40 (d, 1H, CH_2, J_{HH} = 15.0 Hz), 2.97 (d, 1H, CH_2, J_{HH} = 15.0 Hz), 2.01 (s, 15H, Cp*), 1.09 (s, 9H, $C(CH_3)_3$)	288.00 (CO), 111.56 ($C_5(CH_3)_5$), 54.41 (CH_2), 33.69 ($C(CH_3)_3$), 29.84 ($C(CH_3)_3$), 10.11 ($C_5(CH_3)_5$)
8	3.00 (d, 2H, CH_2, J_{HH} = 18.0 Hz), 2.57 (d, 2H, CH_2, J_{HH} = 18.0 Hz), 1.64 (s, 15H, Cp*), 1.33 (s, 9H, $NC(CH_3)_3$), 1.00 (s, 9H, $CH_2C(CH_3)_3$)	*b*
8′^{e}	3.52 (d, 1H, CH_2, J_{HH} = 12.6 Hz), 2.85 (d, 1H, CH_2, J_{HH} = 12.6 Hz), 1.90 (s, 15H, Cp*), 1.48 (s, 9H, $NC(CH_3)_3$), 1.08 (s, 9H, $CH_2C(CH_3)_3$)	207.53 (CN), 110.73 ($C_5(CH_3)_5$), 63.44 ($C(CH_3)_3$), 41.66 (CH_2), 32.99 ($C(CH_3)_3$), 30.10 ($C(CH_3)_3$), 29.77 ($C(CH_3)_3$), 10.12 ($C_5(CH_3)_5$)
9^f	2.50 (s, 3H, CH_3CN), 1.80 (s, 15H, Cp*), 1.30 (d, 1H, CH_2, J_{HH} = 10.5 Hz), 1.08 (s, 9H, $C(CH_3)_3$), 0.70 (d, 1H, CH_2, J_{HH} = 10.5 Hz)	CH_3CN not observed, 113.67 ($C_5(CH_3)_5$), 66.52 (CH_2), 38.80 ($C(CH_3)_3$), 34.25 ($C(CH_3)_3$), 9.31 ($C_5(CH_3)_5$), 4.29 (CH_3CN)
9′^{f}	3.02 (br, 3H, CH_3CN), 2.70 (br, 3H, CH_3CN), 2.22 (s, 15H, Cp*), 1.53 (d, 1H, CH_2, J_{HH} = 12.0 Hz), 1.42 (s, 9H, $C(CH_3)_3$), 0.52 (d, 1H, CH_2, J_{HH} = 12.0 Hz)	CH_3CN not observed, 111.64 ($C_5(CH_3)_5$), 56.62 (CH_2), 37.79 ($C(CH_3)_3$), 34.91 ($C(CH_3)_3$), 9.23 ($C_5(CH_3)_5$), 4.88 (br, CH_3CN), 3.55 (br, CH_3CN)
10′^{c,e}	2.90 (d, 1H, CH_2, J_{HH} = 16.7 Hz), 2.44 (d, 1H, CH_2, J_{HH} = 16.7 Hz), 1.94 (s, 15H, Cp*), 1.51 (d, 9H, J_{HP} = 9.9 Hz, $P(CH_3)_3$), 0.896 (s, 9H, $C(CH_3)_3$)	264.6 (d, J_{CP} = 8.0 Hz, CO), 111.4 ($C_5(CH_3)_5$), 69.82 (CH_2), 54.36 ($C(CH_3)_3$), 29.96 ($C(CH_3)_3$), 11.71 (d, J_{CP} = 32.0 Hz, $P(CH_3)_3$), 10.23 ($C_5(CH_3)_5$)
11^{c,e}	2.88 (vt, 1H, $C_5Me_4CH_2$, J = 3.0 Hz), 2.72 (dd, 1H, $C_5Me_4CH_2$, J = 2.7, 13.2 Hz), 1.93 (d, 3H, Me, J = 2.4 Hz), 1.73 (d, 3H, Me, J = 3.3 Hz), 1.69 (s, 3H, Me), 1.40 (d, 9H, $P(CH_3)_3$, J_{HP} = 7.8 Hz), 1.17 (d, 3H, Me, J_{HP} = 3.6 Hz), 0.99 (s, 9H, $C(CH_3)_3$), 0.87 (m, 1H, CH_2CMe_3), 0.34 (d, 1H, CH_2CMe_3, J = 12.9 Hz)	131.00 ($C_5Me_4CH_2$), 110.16 ($C_5Me_4CH_2$), 108.36 ($C_5Me_4CH_2$), 107.29 (d, $C_5Me_4CH_2$, J_{CP} = 8.0 Hz), 104.36 ($C_5Me_4CH_2$), 64.85 (d, CH_2CMe_3, J_{CP} = 6.5 Hz), 53.94 ($C_5Me_4CH_2$, J_{CP} = 10.4 Hz), 39.26 (d, CH_2CMe_3, J_{CP} = 14.2 Hz), 35.19 ($C(CH_3)_3$), 16.76 (d, $P(CH_3)_3$, J_{CP} = 25.0 Hz), 12.82 (d, $C_5(CH_3)_4CH_2$, J_{CP} = 26.8 Hz), 11.20 ($C_5(CH_3)_4CH_2$, J_{CP} = 19.5 Hz), 9.92 ($C_5(CH_3)_4CH_2$), 9.02 ($C_5(CH_3)_4CH_2$, J_{CP} = 30.7 Hz)
11′^{c,e}	2.75 (vt, 1H, $C_5Me_4CH_2$, J = 3.6 Hz), 2.60 (dd, 1H, $C_5Me_4CH_2$, J = 3.6, 13.2 Hz), 1.98 (d, 3H, Me, J_{HP} = 2.1 Hz), 1.86 (s, 3H, Me), 1.74 (s, 3H, Me), 1.53 (d, 9H, $P(CH_3)_3$, J_{HP} = 8.4 Hz), 1.31 (d, 3H, Me, J_{HP} = 3.3 Hz), 1.01 (s, 9H, $C(CH_3)_3$), 0.87 (dd, 1H, CH_2CMe_3, J = 23.7, 13.8 Hz), 0.34 (dd, 1H, CH_2CMe_3, J = 13.8, 2.4 Hz)	131.06 ($C_5Me_4CH_2$), 108.66 ($C_5Me_4CH_2$), 105.15 (d, $C_5Me_4CH_2$, J_{CP} = 8.0 Hz), 103.28 ($C_5Me_4CH_2$), 102.49 ($C_5Me_4CH_2$), 47.51 (d, $C_5Me_4CH_2$, J_{CP} = 8.0 Hz), 37.23 (d, CH_2CMe_3, J_{CP} = 3.0 Hz), 36.74 (d, CH_2CMe_3, J_{CP} = 8.1 Hz), 35.37 ($C(CH_3)_3$), 16.54 (d, $P(CH_3)_3$, J_{CP} = 30.0 Hz), 11.24 ($C_5(CH_3)_4CH_2$), 11.15 ($C_5(CH_3)_4CH_2$), 9.39 ($C_5(CH_3)_4CH_2$), 8.62 ($C_5(CH_3)_4CH_2$)

[a] In THF-d_8. [b] Not recorded. [c] ^{31}P NMR (δ, ppm): **5** = 6.38 (s); **5′**^{e} = –4.34 (s), J_{PW} = 191 Hz; **10′**^{e} = –4.33 (s), J_{PW} = 187 Hz; **11** = –2.89 (s); **11′**^{e} = –21.88 (s), J_{PW} = 345 Hz. [d] In THF-d_8 at –100 °C. [e] In $CDCl_3$. [f] In CD_2Cl_2.

seconds they became bright yellow as yellow powders precipitated. The reaction vessels were sealed, removed from the drybox, and reattached to a vacuum line. The solvent and excess isocyanide were removed in vacuo. The yellow residues were dissolved in a minimum of Et_2O and placed in a freezer (–30 °C). The desired product complexes crystallized overnight in nearly quantitative yields as microcrystalline yellow needles. The needles were dried in vacuo after the mother liquors had been removed by cannulation.

Preparation of [$Cp^*Mo(NO)(CH_2CMe_3)(NCMe)$]$BF_4$ (9). $Cp^*Mo(NO)(CH_2CMe_3)Cl$ (331 mg, 0.900 mmol) and $AgBF_4$ (175 mg, 0.897 mmol) were intimately mixed in a Schlenk tube. The tube was cooled to −60 °C and MeCN (10 mL) was slowly added such that it froze upon entering the tube. The tube and its contents were then warmed to −20 °C whereupon a color change from purple to red-brown occurred and a white precipitate formed. The precipitate was removed by filtration through Celite (2 × 2 cm) supported on a glass frit. The filtrate was reduced to an oil in vacuo. First Et_2O (50 mL) and then pentane (2 × 30 mL) were used to triturate the oil into a tractable yellow powder which was dried in vacuo for 24 h. The powder was dissolved in a minimum of CH_2Cl_2 (~3 mL), and Et_2O (30 mL) was added to the amber solution. Filtration of this solution through Celite (1 × 4 cm) followed by cooling of the filtrate to −60 °C for 4 h afforded **9** as irregular orange-yellow crystals.

Preparation of $[Cp^*W(NO)(CH_2CMe_3)(NCMe)_2]BF_4$ (9′). A solution of $Cp^*W(NO)(CH_2CMe_3)Cl$ (400 mg, 0.879 mmol) in MeCN (10 mL) at −10 °C was cannulated into a stirred slurry of $AgBF_4$ (170 mg, 0.871 mmol) in MeCN (5 mL). The mixture became orange immediately upon mixing. The reaction mixture was filtered through Celite (2 × 2 cm), and the filtrate was concentrated in vacuo to 5 mL. Et_2O (5 mL) was added to the MeCN solution, and the resulting mixture was placed in a freezer overnight to induce crystallization. Orange crystals of **9′** were isolated the next morning by removing the mother liquor with a cannula.

Reaction of $Cp^*Mo(NO)(C\{O\}CH_2CMe_3)Cl$ (7) with PMe_3: Generation of $[Cp^*Mo(NO)(C\{O\}\{PMe_3\}CH_2CMe_3)(PMe_3)]Cl$. An NMR tube was charged with a $CDCl_3$ solution of **7** (15 mg). An initial ^1H NMR spectrum was recorded.[15] Excess PMe_3 was then vacuum-transferred into the NMR tube. No visible color change occurred, but a ^1H NMR spectrum revealed that all of complex **7** had been consumed and a single product complex had been formed. The product was formulated as $[Cp^*Mo(NO)(C\{O\}\{PMe_3\}CH_2CMe_3)(PMe_3)]Cl$.

Spectroscopic data for $[Cp^*Mo(NO)(C\{O\}\{PMe_3\}CH_2CMe_3)(PMe_3)]Cl$: ^1H NMR (C_6D_6) δ 2.15 (dd, 1 H, CH_2, $^2J_{HH} = 15.0$ Hz, $^3J_{HP} = 6.9$ Hz), 1.84 (s, 15 H, $C_5(CH_3)_5$), 1.76 (dd, 9 H, PMe_3, $^2J_{HP} = 12.9$ Hz, $^3J_{PP} < 1$ Hz), 1.63 (dd, 1 H, CH_2, $^2J_{HH} = 15.0$ Hz, $^3J_{HP} = 28.5$ Hz), 1.43 (dd, 9 H, PMe_3, $^2J_{HP} = 9.9$ Hz, $^3J_{PP} < 1$ Hz), 0.84 (s, 9 H, $C(CH_3)_3$).

All attempts to isolate this product complex have failed to date. For example, removal of the solvent in vacuo yielded a white powder. The powder did not completely redissolve in $CDCl_3$, CD_2Cl_2, or C_6D_6. A ^1H NMR spectrum of the portion that did dissolve revealed the presence of a multitude of compounds, none of which were **7** or the putative $[Cp^*Mo(NO)(C\{O\}\{PMe_3\}CH_2CMe_3)(PMe_3)]Cl$.

Reaction of $Cp^*W(NO)(\eta^2\text{-}C\{O\}CH_2CMe_3)Cl$ (7′) with PMe_3: Preparation of $Cp^*W(NO)(\eta^1\text{-}C\{O\}CH_2CMe_3)(PMe_3)Cl$ (10′). To a rapidly stirred solution of $Cp^*W(NO)(\eta^2\text{-}C\{O\}CH_2CMe_3)Cl$ (120 mg, 0.248 mmol) in Et_2O (20 mL) was introduced PMe_3 (1 atm) whereupon an immediate color change from yellow to orange occurred. The final orange solution was taken to dryness in vacuo. The remaining residue was extracted with Et_2O (3 × 30 mL) and filtered through Celite (2 × 2 cm) supported on a glass frit. Cooling of the filtrate to −30 °C overnight afforded orange crystals of the desired product complex. Concentration and cooling of the mother liquor yielded another fraction of **10′**.

Reaction of $Cp^*Mo(NO)(CH_2CMe_3)(PMe_3)Cl$ (5) with LDA: Preparation of $(\eta^5,\eta^1\text{-}C_5Me_4CH_2)Mo(NO)(CH_2CMe_3)(PMe_3)$ (11). $Cp^*Mo(NO)(CH_2CMe_3)(PMe_3)Cl$ (900 mg, 2.03 mmol) and LDA (220 mg, 2.06 mmol) were combined in a Schlenk tube and THF (25 mL) was vacuum-transferred onto the solids at −196 °C. The rapidly stirred reaction mixture was then warmed to room temperature, and the solvent was removed in vacuo. The oily brown residue was dried in vacuo for 6 h and then was suspended in Et_2O (50 mL) and filtered through neutral alumina I (2 × 3 cm) supported on a glass frit. The alumina column was washed with Et_2O until the amber band had been completely eluted. Solvent was removed from the combined filtrates in vacuo, and the yellow residue was extracted with pentane (50 mL). The pentane extract was filtered through Celite (1 × 2 cm) supported on a frit, concentrated in vacuo, and cooled to induce crystallization. After a week at −30 °C, amber crystals of complex **11** were isolated by removing the mother liquor via cannulation.

Reaction of $Cp^*W(NO)(CH_2CMe_3)(PMe_3)Cl$ (5′) with LDA: Preparation of $(\eta^5,\eta^1\text{-}C_5Me_4CH_2)W(NO)(CH_2CMe_3)(PMe_3)$ (11′). Into a rapidly stirred solution of $Cp^*W(NO)(CH_2CMe_3)(PMe_3)Cl$ (500 mg, 0.940 mmol) in THF (20 mL) (ν_{NO} 1566 cm^{-1}) was cannulated a slurry of LDA (100 mg, 0.935 mmol) in THF (10 mL). The mixture was stirred for 2 h at room temperature during which time the reaction mixture darkened from orange to red-orange (ν_{NO} 1557 cm^{-1}). The solvent was removed from the final reaction mixture in vacuo, and the residue was extracted with Et_2O (5 × 20 mL). The combined extracts were filtered through neutral alumina I (2 × 3 cm) supported on a glass frit. The yellow filtrate was concentrated and maintained at −30 °C for 1 week to induce the crystallization of **11′** as a yellow powder. More product was isolated from the mother liquor by repeated concentrations and coolings. X-ray quality crystals of **11′** were obtained by recrystallization of the yellow powder from benzene/hexanes (1:1).

X-ray Crystallographic Analyses of $Cp^*Mo(NO)(\eta^2\text{-}C\{O\}CH_2CMe_3)Cl$ (7) and $(\eta^5,\eta^1\text{-}C_5Me_4CH_2)W(NO)(CH_2CMe_3)(PMe_3)$ (11′). Crystallographic data for complexes **7** and **11′** appear in Table VI. The final unit-cell parameters were obtained by least-squares analysis on the setting angles for 25 reflections with $2\theta = 47.5\text{–}54.1°$ for **7** and 25.0–27.9° for **11′**. The intensities of three standard reflections, measured every 200 reflections throughout the data collections, remained constant for **7** and decreased uniformly by 3.4% for **11′**. The data were processed[16] and corrected for Lorentz and polarization effects, decay (for **11′**), and absorption (empirical, based on azimuthal scans for three reflections).

Both structures were solved by heavy-atom methods, the coordinates of the heavy atoms being determined from the Patterson functions and those of the remaining non-hydrogen atoms from subsequent difference Fourier syntheses. The asymmetric unit of **7** consists of two molecules. All non-hydrogen atoms of both complexes were refined with anisotropic thermal parameters. Hydrogen atoms were fixed in idealized positions (C–H = 0.98 Å, $B_H = 1.2B_{\text{bonded atom}}$). Neutral-atom scattering factors for all atoms and anomalous dispersion corrections for the non-hydrogen atoms were taken from ref 17. A parallel refinement of the mirror-image structure of **11′** resulted in substantially higher residuals, the R and R_w factor ratios being 1.37 and 1.20, respectively. Final atomic coordinates and equivalent isotropic thermal parameters, selected bond lengths, and selected bond angles appear in Tables VII–IX, respectively. Hydrogen atom parameters, anisotropic thermal parameters, complete tables of bond lengths and bond angles, torsion angles, intermolecular contacts, and least-squares planes are included as supplementary material. Views of the solid-state molecular structures of complexes **7** and **11′** are displayed in Figures 1 and 2, respectively.

Results and Discussion

Synthesis and Properties of the Complexes $Cp^*M(NO)(CH_2CMe_3)Cl$ and $Cp^*M(NO)(CH_2CMe_3)_2$ [M = Mo, W] (1,1′,2,2′). For a number of years we had been unable to synthesize cleanly the 16-valence-electron $Cp'W(NO)(R)Cl$ complexes from their dichloro precursors.[18] Indeed, only recently did we communicate our first successful synthesis of $Cp^*W(NO)(CH_2SiMe_3)Cl$ from

---

[15] ^1H NMR data for **7** in $CDCl_3$: δ 3.45 (d, 1 H, CH_2, $J_{HH} = 15.9$ Hz), 3.06 (d, 1 H, CH_2, $J_{HH} = 15.9$ Hz), 1.95 (s, 15 H, $C_5(CH_3)_5$), 1.23 (s, 9 H, $C(CH_3)_3$).

[16] TEXSAN/TEXRAY structure analysis package, Version 5.1. Molecular Structure Corp., 1985.

[17] *International Tables for X-ray Crystallography*, Kynoch Press: Birmingham, U.K. (present distributor Kluwer Academic Publishers: Dordrecht, The Netherlands), 1974; Vol. IV, pp 99–102 and 149.

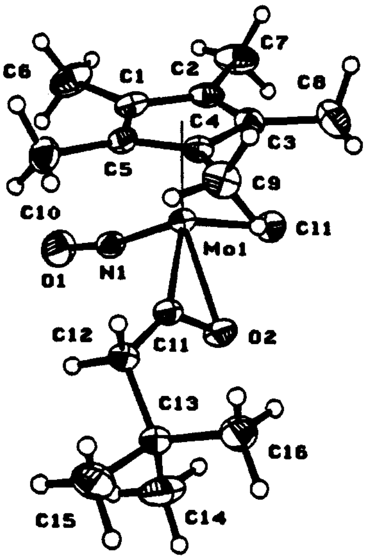

Figure 1. View of one of the two independent molecules of $Cp^*Mo(NO)(\eta^2\text{-}C\{O\}CH_2CMe_3)Cl$ (7); 33% probability thermal ellipsoids are shown for the non-hydrogen atoms.

$Cp^*W(NO)(CH_2SiMe_3)_2$, albeit via a somewhat indirect route (eq 1).[7]

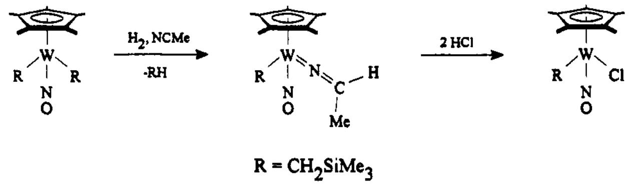

(1)

However, this route is not particularly appealing synthetically, since the yield of $Cp^*W(NO)(CH_2SiMe_3)Cl$ from the customary starting material, $Cp^*W(NO)Cl_2$, is only 30% overall after the three-step conversion involved. Nevertheless, we were intrigued by the air and thermal stability of monomeric $Cp^*W(NO)(CH_2SiMe_3)Cl$ which indicated that it was our previous methodology rather than any intrinsic instability that had thwarted our attempts to prepare this class of molecules. Having also recently discovered synthetic methodology leading to the very sensitive and reactive $Cp'M(NO)(aryl)_2$ complexes (eq 2),[10] we decided to investigate whether this new methodology could be utilized for the preparation of the desired monoalkyl complexes.

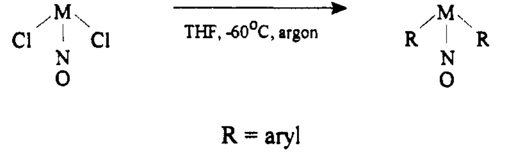

(2)

The synthesis of $Cp^*W(NO)(CH_2CMe_3)Cl$ using this new methodology has been reported in connection with a related study,[8] but the preparation of its new molybdenum congener merits some comment. The transformation leading to $Cp^*Mo(NO)(CH_2CMe_3)Cl$ is portrayed in eq 3.

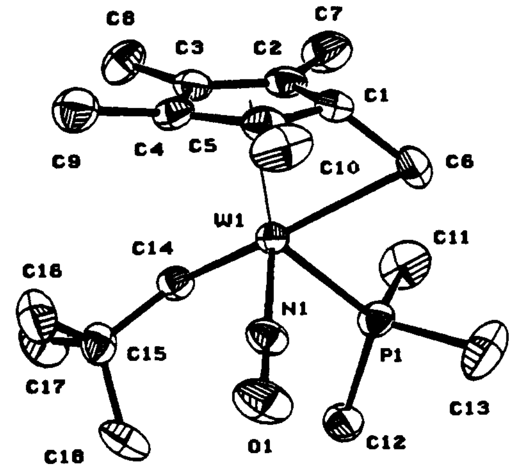

Figure 2. View of $(\eta^5,\eta^1\text{-}C_5Me_4CH_2)W(NO)(CH_2CMe_3)(PMe_3)$ (11′); 33% probability thermal ellipsoids are shown for the non-hydrogen atoms.

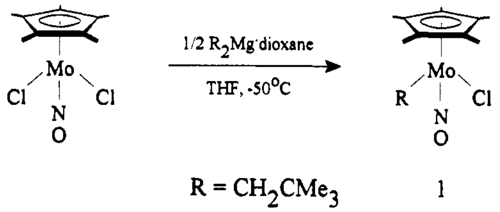

(3)

The conversion is generally similar to the tungsten case, but the control of temperature is extremely critical for the success of reaction 3. Above −45 °C, the desired complex reacts further with $(Me_3CCH_2)_2Mg\cdot X$(dioxane) to produce $Cp^*Mo(NO)(CH_2CMe_3)_2$ and unused starting material. Since $Cp^*Mo(NO)Cl_2$ is nearly insoluble in cold THF, extended reaction times are required to achieve solutions of $Cp^*Mo(NO)(CH_2CMe_3)Cl$ uncontaminated by $Cp^*Mo(NO)(CH_2CMe_3)_2$. It should be noted that it is nearly impossible to isolate pure monoalkylated product from mixtures of the mono- and dialkyl complexes. Finally, the $Cp^*Mo(NO)Cl_2$ starting material *must* be highly pure in order to obtain a clean metathesis.[19]

Fortunately, it is not always necessary to isolate the $Cp^*M(NO)(CH_2CMe_3)Cl$ complexes when investigating their further reactivity. Indeed, during this work, we often generated them in situ, filtered the reaction solutions to remove the $MgCl_2$·dioxane byproduct, and then added the next solvent or reagent directly. Typical yields of the monoalkyl complexes generated in this manner are in the range of 90 ± 5%.

The solid-state molecular structure of $Cp^*W(NO)(CH_2SiMe_3)Cl$ is that of a three-legged piano stool,[5] and we have no reason to suspect that either of the neopentyl analogues (1 and 1′) is anything but monomeric. Thus, in solution and the solid-state, both complexes are purple and exhibit strong ν_{NO} bands in their Nujol mull IR spectra (1 = 1606 cm^{-1}; 1′ = 1582 cm^{-1}) in the same energy range (1650–1550 cm^{-1}) as their monomeric dialkyl and diaryl analogues. The ^1H NMR spectra of 1 and 1′ are also consistent with their formulations. The spectra display two doublets at markedly different chemical shifts at-

---

[18] A commentary of our attempts to synthesize such complexes is provided in a paper describing the chemistry of $Cp'M(NO)(\eta^2\text{-benzyl})Cl$ complexes.[12] These monoalkyl derivatives are 18-electron complexes by virtue of their containing three-electron donor benzyl groups. We desired complexes in which the hydrocarbyl ligand did not provide any extra electron density to the coordinatively and electronically unsaturated metal center.

[19] We have found that crude $Cp^*Mo(NO)Cl_2$ prepared from $Cp^*Mo(NO)(CO)_2$ and PCl_5 is best purified by Soxhlet extraction and crystallization from CH_2Cl_2.[11]

Table IV. Electrochemical Data for the First Reduction of $Cp^*M(NO)Cl_2$, $Cp^*M(NO)(CH_2CMe_3)Cl$ (1, 1′), and $Cp^*M(NO)(CH_2CMe_3)_2$ (2, 2′)[a]

compd	scan rate (ν, V s^{-1})	$E^{\circ\prime}{}_1$[b] (mV)	ΔE[c]	$i_{p,a}/i_{p,c}$[d]
$Cp^*Mo(NO)Cl_2$	1.0	−350	194(171)	1.0
	0.6	−350	162(136)	1.0
	0.2	−350	113(94)	1.0
$Cp^*Mo(NO)(CH_2CMe_3)Cl$	1.0	−970	207(230)	1.0
	0.6	−960	172(188)	1.0
	0.2	−970	125(132)	0.9
$Cp^*Mo(NO)(CH_2CMe_3)_2$	1.0	~−1590	510(186)	0.7
$Cp^*W(NO)Cl_2$	1.0	−750	234(167)	1.0
	0.6	−750	178(136)	1.0
	0.2	−740	116(109)	1.0
$Cp^*W(NO)(CH_2CMe_3)Cl$	8.0	~−1220	550	0.7
	4.0	~−1220	360	0.6
	1.0	~−1210	170	0.4
$Cp^*W(NO)(CH_2CMe_3)_2$	1.0	−1720	310(167)	0.9
	0.6	−1700	250(136)	0.8
	0.2	−1680	180(109)	0.8

[a] In THF containing 0.10 M $[n\text{-}Bu_4N]PF_6$, at a Pt-bead working electrode. Potentials are measured vs SCE. [b] Defined as the average of the cathodic and anodic peak potentials. [c] Defined as the separation of the cathodic and anodic peak potentials. Values in brackets are for the Cp_2Fe/Cp_2Fe^+ couple under identical experimental conditions. [d] Ratio of anodic peak current to cathodic peak current.

Table V. Comparative IR and Electrochemical Data in THF

compd	ν_{NO} (cm^{-1})	$E^{\circ\prime}{}_1$ (mV vs SCE at 1.0 V/s)
$Cp^*Mo(NO)Cl_2$	1655	−350[a]
$Cp^*W(NO)Cl_2$	1630	−750[a]
$Cp^*Mo(NO)(CH_2CMe_3)Cl$ (**1**)	1618	−960[a]
$Cp^*W(NO)(CH_2CMe_3)Cl$ (**1′**)	1595	−1210[b]
$Cp^*Mo(NO)(CH_2CMe_3)_2$ (**2**)	1588	−1590[b]
$Cp^*W(NO)(CH_2CMe_3)_2$ (**2′**)	1568	−1700[c]

[a] Reversible. [b] Quasireversible. [c] Reversible at high scan rates, otherwise quasireversible.

tributable to the diastereotopic methylene protons of the neopentyl groups. For example, the methylene protons of the tungsten complex resonate at δ 3.42 and −0.03 ppm, thereby indicating their substantially different magnetic environments in the three-legged piano-stool, i.e. one proton environment is close to the Cl ligand and the other is close to the nitrosyl ligand.

In previous work, we have found that virtually all $Cp'M(NO)X_2$ [X = I, Br, Cl] and $Cp'M(NO)R_2$ [R = alkyl, aryl] complexes exhibit nitrosyl-stretching frequencies in their IR spectra which are indicative of the electron density extant at the metal centers in these compounds.[20] Furthermore, these symmetric complexes exhibit reversible electrochemical reductions in THF or CH_2Cl_2, a feature attributable to the nonbonding nature of the LUMO in these species.[22] Having effected the isolation of the $Cp^*M(NO)(CH_2CMe_3)Cl$ complexes during this work, we are now able to effect a detailed comparison of the complete series of compounds $Cp^*M(NO)Cl_2$, $Cp^*M(NO)(CH_2CMe_3)Cl$, and $Cp^*M(NO)(CH_2CMe_3)_2$ [M = Mo, W] using both IR spectroscopy and electrochemistry. Table V summarizes the results of such a comparison.

As evidenced by the data displayed in Table V, replacement of electronegative chloro ligands with neopentyl groups causes significant shifts in ν_{NO} to lower energy and increases in reduction potential ($E^{\circ\prime}$) to more negative potentials. Consequently, we can conclude that the metal centers in $Cp^*M(NO)(CH_2CMe_3)_2$ are more electron-rich than in their mononeopentyl precursors, which in turn are more electron-rich than in the dichloro complexes. Such a trend is to be expected on the basis of ligand electronegativities. Additionally, in comparing each of the three pairs of compounds, the tungsten complex *always* exhibits the lower ν_{NO} (average of 23 cm^{-1}) and the higher reduction potential (by 400, 260 and 110 mV) than its corresponding molybdenum analogue.

Of these complexes, $Cp^*Mo(NO)(CH_2CMe_3)_2$ and $Cp^*W(NO)(CH_2CMe_3)Cl$ exhibit quasireversible reductions in THF. For exmaple, at a scan rate of 1.0 V/s $Cp^*Mo(NO)(CH_2CMe_3)_2$ exhibits a reduction wave ($i_{p,a}/i_{p,c} = 0.7$) having ΔE almost 3 times that of ferrocene. In contrast, a scan rate of 8.0 V/s is required to achieve a reduction wave having $i_{p,a}/i_{p,c} = 0.7$ for $Cp^*W(NO)(CH_2CMe_3)Cl$. In addition, $Cp^*W(NO)(CH_2CMe_3)_2$ exhibits a reduction wave that approaches reversibility at high scan rates, but is also quasireversible at low scan rates (Table IV).[21] The other three complexes studied exhibit completely reversible reductions as would be expected on the basis of previous studies[10] and calculations.[22]

The general conclusion to emanate from the IR data and the electrochemical reduction potentials is that the molybdenum complexes are more electron-deficient than their tungsten partners. This increased electron-deficiency at the metal center is manifested in the higher reactivity of molybdenum nitrosyl complexes of this type. We have previously established that $Cp^*M(NO)(aryl)_2$ complexes are better Lewis acids than their $Cp^*M(NO)(alkyl)_2$ congeners due to the increased electron-withdrawing ability of aryl groups.[10] The current study indicates that the $Cp^*M(NO)(CH_2CMe_3)Cl$ complexes are comparable in electron-deficiency to the related $Cp^*M(NO)(aryl)_2$ complexes for both the Mo and W systems. For instance, the nitrosyl-stretching frequency of $Cp^*Mo(NO)Ph_2$[10] in THF is 1618 cm^{-1}, only 3 cm^{-1} higher in energy than that exhibited by $Cp^*Mo(NO)(CH_2CMe_3)Cl$. Consistently, from an electrochemical point of view, the reduction potential of $Cp^*W(NO)(p\text{-tolyl})_2$ in THF is −1210 mV[10] and that of $Cp^*W(NO)(CH_2CMe_3)Cl$ is a comparable −1220 mV.

Reactivity of the $Cp^*M(NO)(CH_2CMe_3)Cl$ Complexes with R_2Mg Reagents: Synthesis of Mixed Alkyl and Alkyl Aryl Complexes. We have recently described the synthesis of a variety of asymmetric bis(hydrocarbyl) complexes of tungsten.[8] In this paper we report the preparation of two mixed complexes of molybdenum and two previously unreported mixed complexes of tungsten. Specifically, using similar methodology to that which provided us with diaryl complexes of Mo and W, we have now prepared $Cp^*Mo(NO)(CH_2CMe_3)(CH_2SiMe_3)$ (**3**), $Cp^*W(NO)(CH_2CMe_3)(CH_2CMe_2Ph)$ (**3′**), and $Cp^*M(NO)(CH_2CMe_3)(p\text{-tolyl})$ (**4** and **4′**) (eq 4).

The spectroscopic properties of these mixed complexes are again consistent with their formulations. As one might

---

[20] The degree of $M(d\pi)$–$NO(\pi^*)$ backbonding in a metal–nitrosyl complex is a direct function of the amount of electron density at the metal center in the compound. Transfer of electron density into the $NO(\pi^*)$ antibonding orbital decreases the N–O bond order and thus decreases the nitrosyl stretching frequency (ν_{NO}) as measured in the IR spectrum of the complex.

[21] For moderate charge-transfer rates, quasireversible electrochemical behavior is often observed. The slowness of electron transfer is often ascribed to subtle structural changes that occur upon reduction (or oxidation). For a general description of this phenomenon, see: Geiger, W. E. *Prog. Inorg. Chem.* **1984**, 275. For more detailed descriptions of electrochemical quasireversibility, see (a) Matsuda, H.; Ayabe, Y. *Z. Elektrochem.* **1955**, *59*, 494. (b) Bard, A. J.; Faulkner, L. F. *Electrochemical Methods*; John Wiley and Sons: New York, 1980; Chapter 6.

[22] Legzdins, P.; Rettig, S. J.; Sánchez, L.; Bursten, B. E.; Gatter, M. G. *J. Am. Chem. Soc.* **1985**, *107*, 1411.

$$\mathrm{Cp^*M(NO)(CH_2CMe_3)Cl} + {}^1/{}_2\mathrm{R_2Mg} \rightarrow \mathrm{Cp^*M(NO)(CH_2CMe_3)R} \quad (4)$$

$\mathrm{R} = \mathrm{CH_2SiMe_3}$ (**3**, M = Mo), $\mathrm{CH_2CMe_2Ph}$ (**3′**, M = W), *p*-tolyl (**4**, M = Mo; **4′**, M = W)

expect, the IR nitrosyl-stretching frequencies of the complexes are essentially the average of their symmetric congeners. For example, $\mathrm{Cp^*Mo(NO)(CH_2CMe_3)}$(*p*-tolyl) (**4**) in THF has a ν_{NO} of 1600 cm^{-1} which is within 2 cm^{-1} of the average for $\mathrm{Cp^*Mo(NO)}$(*p*-tolyl)$_2$ (1609 cm^{-1}) and $\mathrm{Cp^*Mo(NO)(CH_2CMe_3)_2}$ (1588 cm^{-1}). An interesting spectral feature appears in the ^{1}H NMR spectra of **3** and **3′**. The signal of one methylene proton of each alkyl group is not only coupled to its partner as expected, but is also weakly coupled to one proton on the other alkyl group (for **3**, $^4J_{HH}$ = 1.8 Hz; for **3′**, $^4J_{HH}$ = 3.0 Hz). Such a phenomenon has been referred to as W-coupling in organic chemistry.[23]

Unsymmetrical bis(hydrocarbyl) complexes of the transition metals have been utilized to study the comparative reactivity of two different metal–carbon bonds at the same transition-metal center. The insertions of CO into the Zr–C bonds of $\mathrm{Cp_2Zr(R)R'}$,[24] the W–C bonds of $\mathrm{Cp^*W(NO)(R)R'}$,[8] and the Ir–C bonds of (η^5-indenyl)$\mathrm{Ir(PMe)_3(R)R'}$[25] have been shown to be regioselective. Thermal eliminations of RH from $\mathrm{Cp^*_2Th(R)R'}$[9f] and $\mathrm{(Me_3P)_4Ru(R)R'}$[9d] are also regioselective and lead to the formation of metallacyclic and benzyne complexes, respectively. Future studies in our laboratories will center on the comparative reactivity of the two different M–C bonds in the Lewis acids, $\mathrm{Cp^*M(NO)(R)R'}$, and their use in asymmetric syntheses.

Reactivity of $\mathrm{Cp^*M(NO)(CH_2CMe_3)Cl}$ with Lewis Bases. Just like the related 16-electron $\mathrm{Cp^*W(NO)(alkyl)_2}$ complexes, the mononeopentyl compounds prepared in this work are very reactive toward Lewis bases. The coordinative and electronic unsaturation of the metal centers in the $\mathrm{Cp^*M(NO)(CH_2CMe_3)Cl}$ complexes is satisfied by coordination of the Lewis base. For example, the addition of $\mathrm{PMe_3}$ to solutions of $\mathrm{Cp^*M(NO)(CH_2CMe_3)Cl}$ causes an immediate color change from purple to yellow and formation of the 1:1 metal-centered adducts **5** and **5′**. The 18-electron phosphine adducts exhibit ^{1}H NMR spectra that are diagnostic of a 4-legged piano-stool molecular structure having the $\mathrm{PMe_3}$ ligand trans to the nitrosyl group. This stereochemistry is best indicated by the Newman projection down the metal–Cp* centroid axis shown below. The methylene protons of the alkyl group are positioned such that H_A is transoidal to the P nucleus ($^3J_{HP}$ = 3.3 Hz for Mo, 4.2 Hz for W) and H_B is cisoidal to the P nucleus ($^3J_{HP}$ = 0 Hz for Mo and W). Since molecular-orbital calculations and X-ray crystallographic analyses have indicated that the vacant coordination site in all 16-electron complexes of the type $\mathrm{Cp'M(NO)(Y)(Z)}$ [Y, Z = 1-electron ligand] is trans to the NO group,[22] it is not surprising that the $\mathrm{PMe_3}$ enters the metals' coordination spheres at this position. The adduct isomers isolated appear to be the thermodynamically favored ones since they exhibit no tendency to isomerize upon warming.

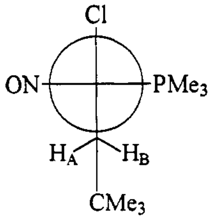

The addition of $\mathrm{PMe_3}$ to the chloro neopentyl complexes causes a drop in the IR nitrosyl-stretching frequencies of 31 cm^{-1} (Mo) and 29 cm^{-1} (W), a feature consistent with the metal centers in the adducts becoming more electron-rich. Prolonged exposure of complexes **5** and **5′** to high vacuum does not effect the dissociation of the phosphine ligand, as occurs for $\mathrm{CpW(NO)(CH_2SiMe_3)_2(PMe_3)}$.[26] This fact is consistent with our conclusion (vide supra) that the chloro neopentyl complexes are about as electron-deficient at their metal centers as are the related diaryl complexes which also bind $\mathrm{PMe_3}$ irreversibly.[10] Interestingly, a bulkier base such as pyridine also coordinates to the $\mathrm{Cp^*M(NO)(CH_2CMe_3)Cl}$ complexes, but in a reversible fashion (eq 5). At low temperatures the pyridine adducts

$$\mathrm{Cp^*M(NO)(CH_2CMe_3)Cl} \underset{-\mathrm{py}}{\overset{+\mathrm{py}}{\rightleftharpoons}} \underset{\mathbf{6,6'}}{\mathrm{Cp^*M(NO)(CH_2CMe_3)(Cl)(py)}} \quad (5)$$

are relatively stable and may be crystallized from $\mathrm{Et_2O}$ solutions containing an excess of pyridine. As solids, the isolated adducts have a tendency to lose pyridine under vacuum. Dissolution of either **6** or **6′** in a noncoordinating solvents such as $\mathrm{CDCl_3}$, $\mathrm{C_6D_6}$, or a coordinating solvent such as THF-d_8 causes quantitative dissociation into pyridine and starting material as evidenced by ^{1}H NMR spectroscopy. $\mathrm{CDCl_3}$ proved to have an insufficiently low freezing point to enable spectroscopic characterization of either pyridine adduct. However, these complexes were characterized spectroscopically by low-temperature NMR studies in THF-d_8 (Table III). As a solution of either pyridine adduct is cooled, signals due to the methylene protons of the neopentyl group are the first to coalesce (−30 °C Mo; −20 °C W), presumably due to the slowed rotation of the alkyl ligand about the metal–carbon bond. At lower temperatures (−75 °C for Mo; −60 °C for W) the methyl proton resonances of the Cp* rings coalesce. At even lower temperatures, the pyridine in the sample begins to coordinate to the metal centers, and all signals begin to sharpen. Finally, at −100 °C only signals attributable to the pyridine complexes **6** and **6′** are evident. At this temperature, the samples are orange (characteristic of **6** and **6′**) and not purple (characteristic of **1** and **1′**).

Lewis-base substrates containing unsaturated linkages initially form adducts with the $\mathrm{Cp^*M(NO)(CH_2CMe_3)Cl}$ complexes, but undergo subsequent facile insertion into the metal–neopentyl bond. Thus, the reactions of $\mathrm{Cp^*M(NO)(CH_2CMe_3)Cl}$ with CO or $\mathrm{CNCMe_3}$ provide the acyl (**7**, **7′**) and iminoacyl (**8**, **8′**) complexes (eq 6). Typically, the molybdenum complex reacts faster or at a lower temperature than does $\mathrm{Cp^*W(NO)(CH_2CMe_3)Cl}$,

---

[23] Jackman, L. M.; Sternhell, S. *Applications of Nuclear Magnetic Resonance Spectroscopy in Organic Chemistry*, 2nd ed.; Pergamon Press: Toronto, 1969; p 334.

[24] (a) Lappert, M. F.; Jeffery, J.; Luong-Thi, N. T.; Webb, M.; Atwood, J. L.; Hunter, W. E. *J. Chem. Soc., Dalton Trans.* 1981, 1594. (b) Erker, G. *Acc. Chem. Res.* **1984**, *17*, 103 and refs therein.

[25] Foo, T.; Bergman, R. G. *Organometallics* **1992**, *11*, 1811.

[26] Legzdins, P.; Rettig, S. J.; Sánchez, L. *Organometallics* **1988**, *7*, 2394.

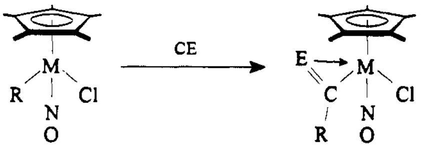

(6)

E = O (7, 7'); E = NCMe$_3$ (8, 8')

R = CH$_2$CMe$_3$

this feature being another manifestation of the greater electron-deficiency of the molybdenum center. The isolated yield of 7 (30%) is substantially lower than that of 8 (95%) primarily due to the complex nature of the CO reaction for the molybdenum case.[27] In contrast, the reaction with *tert*-butyl isocyanide is facile and very clean. Thus, addition of CNCMe$_3$ to a purple Et$_2$O solution of Cp*Mo(NO)(CH$_2$CMe$_3$)Cl causes an immediate color change to amber (presumably due to the adduct Cp*Mo(NO)(CH$_2$CMe$_3$)(CNCMe$_3$)Cl) followed by a color change to yellow and precipitation of the inserted species, Cp*Mo(NO)(η^2-C{NCMe$_3$}CH$_2$CMe$_3$)Cl (8).

In accord with other acyl complexes that we have previously isolated,[8,28] the neopentyl–acyl complexes prepared in this work contain classic η^2-acyl ligands.[29] The IR spectrum of 7 as a Nujol mull, for example, exhibits two strong bands at 1624 and 1601 cm^{-1} attributable to the terminal nitrosyl and η^2-acyl ligands, but unambigous assignment of these bands is not possible without labeling studies. To confirm the nature of the acyl group in 7, the complex was subjected to an X-ray crystallographic analysis. Experimental parameters for this analysis are collected in Table VI, and selected intramolecular bond lengths and angles are located in Table VIII. An ORTEP diagram of 7 clearly showing the η^2-acyl ligand is shown in Figure 1. The two independent molecules of 7 that were crystallographically determined exhibit short Mo–O bond lengths of 2.217(2) and 2.226(2) and very acute C(11)–Mo–O(2) bond angles of 32.9(1) and 33.3(1)°, respectively. The difference between the Mo–O(2) and Mo–C(11) bond lengths of 0.153 and 0.182 Å is diagnostic of an η^2-acyl ligand.[29] A nearly isostructural analogue of complex 7, namely CpMo(NO)(η^2-C{O}-*p*-tolyl)I, has been previously prepared by Hersh.[30] Consistently, this latter complex exhibits a Δ[(Mo–O)–(Mo–C)] of 0.163 Å. As of 1988,[29] the known range of Δ[(Mo–O)–(Mo–C)] for structurally characterized η^2-acyl complexes was 0.17–0.30 Å. Both the Hersh complex and complex 7 are slightly outside of this range. The low values of Δ[(Mo–O)–(Mo–C)] observed for these two complexes are more similar to electron-deficient Group 4 η^2-acyl complexes and is likely a function of the Lewis acidic metal centers in these compounds.

Table VI. Crystallographic and Experimental Data for the Complexes 7 and 11′[a]

	7	11′
formula	C$_{16}$H$_{26}$NO$_2$ClMo	C$_{18}$H$_{34}$NOPW
fw	395.78	495.30
color	yellow, prism	orange, needle
cryst dimens (mm^3)	0.35 × 0.40 × 0.40	0.12 × 0.12 × 0.40
cryst syst	monoclinic	orthorombic
space group	$P2_1/n$ (No. 14)	$P2_12_12_1$ (No. 19)
a (Å)	15.226(2)	14.323(1)
b (Å)	12.376(2)	16.861(2)
c (Å)	19.641(2)	8.511(2)
β (deg)	95.921(1)	90
V (Å^3)	3681.3(8)	2055.4(4)
Z	8	4
d_{calcd} (Mg/m^3)	1.428	1.600
$F(000)$	1632	984
μ(Mo Kα) (cm^{-1})	8.45	58.19
T (K)	294	294
transmission factors (relative)	0.97–1.00	0.81–1.00
scan type	ω–2θ	ω–2θ
scan range (deg in ω)	1.57 + 0.35 tan θ	1.25 + 0.35 tan θ
scan speed (deg/min)	32	16
data collected	$+h,+k,\pm l$	$+h,+k,+l$
2θ_{max} (deg)	65	65
crystal decay (%)	negligible	3.4
total no. of rflns	14300	4142
no. of unique rflns	13307	4142
R_{merge}	0.047	–
no. of rflns with $I > 3\sigma(I)$	7215	2420
no. of variables	379	199
R	0.032	0.030
R_w	0.032	0.024
gof	2.16	1.34
max Δ/σ (final cycle)	0.13	0.01
residual density (e/Å^3)	–0.52 to +0.74 (near Mo)	–0.73 to +0.84 (near W)

[a] Rigaku AFC6S diffractometer, Mo Kα radiation ($\lambda_{K\alpha}$ = 0.71069 Å), graphite monochromator, takeoff angle 6.0°, aperture 6.0 × 6.0 mm at a distance of 285 mm from the crystal, stationary background counts at each end of the scan (scan/background time ratio 2:1, up to eight rescans), $\sigma^2(F)^2 = [S^2(C + 4B)]/\mathrm{Lp}^2$ (S = scan rate, C = scan count, B = normalized background count), function minimized $\sum w(|F_o| - |F_c|)^2$ where $w = 4F_o^2/\sigma^2(F_o)^2$, $R = \sum||F_o| - |F_c||/\sum|F_o|$, $R_w = [\sum w(|F_o| - |F_c|)^2/\sum F_o^2]^{1/2}$, and gof $= [\sum w(|F_o| - |F_c|)^2/(\text{no. of degrees of freedom})]^{1/2}$. Values given for R, R_w, and gof are based on those reflections with $I \geq 3\sigma(I)$.

The IR spectra of 8 and 8′ are diagnostic for η^2-iminoacyl moieties. Namely, ν_{CN} at 1715 (Mo) and 1680 (W) cm^{-1} are characteristic of this ligand type.[29] It is of interest to note that the nitrosyl-stretching frequency for the iminoacyl complexes are 50 (Mo) and 47 (W) wavenumbers lower than that of the acyl complexes 7 and 7′. It can therefore be concluded that, for the Cp*M(NO) fragment, an NCMe$_3$ group is a better source of electron density than an oxygen atom.

Reactivity of the Cp*M(NO)(CH$_2$CMe$_3$)Cl Complexes with AgBF$_4$. The chloro ligands in the starting materials are very susceptible to abstraction by Ag(I) salts. Thus, treatment of Cp*M(NO)(CH$_2$CMe$_3$)Cl with AgBF$_4$ in acetonitrile leads to good yields of the 16-electron mono(acetonitrile) molybdenum cation [Cp*Mo(NO)(CH$_2$CMe$_3$)(NCMe)]BF$_4$ (9) or the 18-electron bis(acetonitrile) tungsten cation [Cp*W(NO)(CH$_2$CMe$_3$)(NCMe)$_2$]BF$_4$ (9′) (eq 7). Complexes 9 and 9′ are closely related to other organometallic Mo and W cations that we have previously described.[31] A variety of complexes of

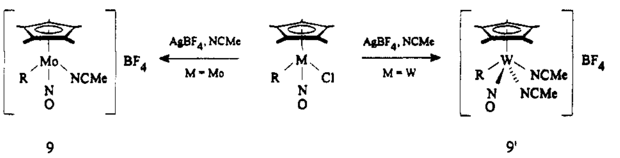

(7)

9 9′

---

[27] After the Cp*Mo(NO)(η^2-C{O}CH$_2$CMe$_3$)Cl product has been crystallized from Et$_2$O, the remaining supernatant solution can be taken to dryness and the residue redissolved in pentane. Cooling of the red pentane solution affords an impure red solid whose ^{1}H NMR spectrum in C$_6$D$_6$ exhibits a plethora of signals attributable to Cp*, CMe$_3$, and CH$_2$ protons. No successful purification of the compounds in this mixture has yet been effected.

[28] Dryden, N. H.; Legzdins, P.; Lundmark, P. J.; Riesen, A.; Einstein, F. W. B. *Organometallics*, in press.

[29] Durfee, L. D.; Rothwell, I. P. *Chem. Rev.* 1988, *88*, 1059.

[30] The route to this complex does not resemble that in which 7 was prepared, see Bonnesen, P. V.; Yau, P. K. L.; Hersh, W. H. *Organometallics* 1987, *6*, 1587.

Table VII. Final Atomic Coordinates (Fractional) and B_{eq} (Å^2) for $Cp^*Mo(NO)(\eta^2\text{-}C\{O\}CH_2CMe_3)Cl$ (7)

atom	*x*	*y*	*z*	B_{eq}[a]
Mo(1)	0.22316(2)	0.07197(2)	0.20004(1)	2.56(1)
Cl(1)	0.10428(5)	−0.05360(7)	0.21484(4)	4.03(4)
O(1)	0.1399(2)	0.2791(2)	0.2302(1)	6.1(1)
O(2)	0.2819(1)	0.0154(2)	0.3018(1)	3.9(1)
N(1)	0.1721(2)	0.1913(2)	0.2252(1)	3.5(1)
C(1)	0.2209(2)	0.1407(3)	0.0893(1)	3.3(1)
C(2)	0.1942(2)	0.0318(3)	0.0824(1)	3.4(1)
C(3)	0.2659(2)	−0.0357(3)	0.1077(1)	3.1(1)
C(4)	0.3381(2)	0.0317(2)	0.1298(1)	2.7(1)
C(5)	0.3099(2)	0.1422(2)	0.1204(1)	2.9(1)
C(6)	0.1696(2)	0.2394(3)	0.0642(2)	5.6(2)
C(7)	0.1066(2)	−0.0081(4)	0.0482(2)	5.5(2)
C(8)	0.2655(2)	−0.1568(3)	0.1074(2)	4.8(2)
C(9)	0.4297(2)	−0.0068(3)	0.1541(2)	3.9(1)
C(10)	0.3655(2)	0.2424(3)	0.1309(2)	4.4(2)
C(11)	0.3255(2)	0.0855(2)	0.2771(1)	3.0(1)
C(12)	0.4068(2)	0.1389(3)	0.3079(1)	3.4(1)
C(13)	0.4535(2)	0.0924(3)	0.3748(2)	3.6(1)
C(14)	0.3928(3)	0.0948(4)	0.4316(2)	6.1(2)
C(15)	0.5336(3)	0.1637(4)	0.3949(2)	6.7(2)
C(16)	0.4830(2)	−0.0231(3)	0.3639(2)	4.7(2)
Mo(1′)	0.21889(2)	0.39223(2)	0.69675(1)	2.56(1)
Cl(1′)	0.10296(5)	0.26163(7)	0.70804(4)	3.94(4)
O(1′)	0.1356(2)	0.5934(2)	0.7407(1)	5.6(1)
O(2′)	0.2820(1)	0.3238(2)	0.7946(1)	4.1(1)
N(1′)	0.1671(2)	0.5078(2)	0.7296(1)	3.3(1)
C(1′)	0.2155(2)	0.4764(3)	0.5902(1)	3.3(1)
C(2′)	0.1871(2)	0.3683(3)	0.5779(1)	3.5(1)
C(3′)	0.2599(2)	0.2983(2)	0.5983(1)	3.3(1)
C(4′)	0.3321(2)	0.3628(3)	0.6234(1)	3.0(1)
C(5′)	0.3040(2)	0.4738(2)	0.6201(1)	3.0(1)
C(6′)	0.1642(2)	0.5776(3)	0.5713(2)	5.1(2)
C(7′)	0.0987(2)	0.3340(4)	0.5434(2)	5.7(2)
C(8′)	0.2598(2)	0.1769(3)	0.5914(2)	5.3(2)
C(9′)	0.4241(2)	0.3213(3)	0.6447(2)	4.6(2)
C(10′)	0.3602(2)	0.5717(3)	0.6355(2)	4.4(2)
C(11′)	0.3211(2)	0.4017(2)	0.7726(2)	3.1(1)
C(12′)	0.4008(2)	0.4585(3)	0.8055(2)	3.6(1)
C(13′)	0.4496(2)	0.4098(3)	0.8708(2)	3.6(1)
C(14′)	0.3879(3)	0.3980(3)	0.9277(2)	5.3(2)
C(15′)	0.5245(3)	0.4869(3)	0.8950(2)	6.4(2)
C(16′)	0.4874(2)	0.2999(3)	0.8552(2)	5.1(2)

[a] $B_{eq} = (^8/_3)\pi^2\sum\sum U_{ij}a_i{}^*a_j{}^*(a_i{\cdot}a_j)$

Table VIII. Selected Bond Lengths (Å) and Bond Angles (deg) with ESD's in Parentheses for $Cp^*Mo(NO)(\eta^2\text{-}C\{O\}CH_2CMe_3)Cl$ (7)

Distances			
Mo(1)–Cl(1)	2.4258(8)	Mo(1′)–Cl(1′)	2.4204(8)
Mo(1)–O(2)	2.217(2)	Mo(1′)–O(2′)	2.226(2)
Mo(1)–N(1)	1.763(3)	Mo(1′)–N(1′)	1.785(3)
Mo(1)–C(1)	2.332(3)	Mo(1′)–C(1′)	2.334(3)
Mo(1)–C(2)	2.359(3)	Mo(1′)–C(2′)	2.353(3)
Mo(1)–C(3)	2.394(3)	Mo(1′)–C(3′)	2.393(3)
Mo(1)–C(4)	2.390(3)	Mo(1′)–C(4′)	2.385(3)
Mo(1)–C(5)	2.318(3)	Mo(1′)–C(5′)	2.318(3)
Mo(1)–C(11)	2.064(3)	Mo(1′)–C(11′)	2.044(3)
Mo(1)–Cp[a]	2.026(2)	Mo(1′)–Cp′	2.023(2)
O(1)–N(1)	1.200(3)	O(1′)–N(1′)	1.192(3)
O(2)–C(11)	1.222(3)	O(2′)–C(11′)	1.235(3)
Angles			
Cl(1)–Mo(1)–O(2)	85.79(6)	Cl(1′)–Mo(1′)–O(2′)	85.45(6)
Cl(1)–Mo(1)–N(1)	98.46(9)	Cl(1′)–Mo(1′)–N(1′)	98.52(8)
Cl(1)–Mo(1)–C(11)	118.7(1)	Cl(1′)–Mo(1′)–C(11′)	118.7(1)
Cl(1)–Mo(1)–Cp	112.5	Cl(1′)–Mo(1′)–Cp′	113.3
O(2)–Mo(1)–N(1)	99.3(1)	O(2′)–Mo(1′)–N(1′)	99.2(1)
O(2)–Mo(1)–C(11)	32.9(1)	O(2′)–Mo(1′)–C(11′)	33.3(1)
O(2)–Mo(1)–Cp	131.7	O(2′)–Mo(1′)–Cp′	131.1
N(1)–Mo(1)–C(11)	92.8(1)	N(1′)–Mo(1′)–C(11′)	91.3(1)
N(1)–Mo(1)–Cp	120.0	N(1′)–Mo(1′)–Cp′	120.2
C(11)–Mo(1)–Cp	112.7	C(11′)–Mo(1′)–Cp′	112.7
Mo(1)–O(2)–C(11)	66.6(2)	Mo(1′)–O(2′)–C(11′)	65.3(2)
Mo(1)–N(1)–O(1)	167.8(2)	Mo(1′)–N(1′)–O(1′)	168.1(2)
Mo(1)–C(11)–O(2)	80.5(2)	Mo(1′)–C(11′)–O(2′)	81.5(2)
Mo(1)–C(11)–C(12)	151.0(2)	Mo(1′)–C(11′)–C(12′)	150.2(2)
O(2)–C(11)–C(12)	128.4(3)	O(2′)–C(11′)–C(12′)	128.1(3)

[a] Here and elsewhere Cp and Cp′ refer to the unweighted centroids of the C(1–5) and C(1′–5′) cyclopentadienyl rings, respectively.

the type $[Cp'M(NO)(X)(NCMe)_2]PF_6$ [X = halide] are isoelectronic and probably isostructural to the tungsten neopentyl cation **9′**. At room temperature in CD_2Cl_2, the ^1H NMR spectrum of the Mo cation in **9** exhibits only one peak for the coordinated nitrile ligand (integrating for three hydrogens) whereas the W cation **9′** exhibits two broad singlets attributable to the two coordinated acetonitrile groups. The ^1H NMR spectrum of the W cation reveals that the two nitrile ligands are magnetically inequivalent and thus cis to one another in the four-legged piano stool molecular structure. Finally, increased-energy ν_{CN} bands (vs free NCMe at 2230 cm^{-1}) at 2316, 2290 cm^{-1} (Mo) and 2319, 2291 cm^{-1} (W) are diagnostic[32] for the presence of N-bound nitrile ligands in these complexes. Whereas, complex **9′** is indefinitely stable in CD_2Cl_2 solution, the molybdenum complex **9** spontaneously decomposes to a mixture of products and free acetonitrile within hours in CD_2Cl_2 at room temperature. Clearly, the nitrile ligand in the 16-electron Mo cation is considerably more labile than the nitrile ligands in the 18-electron W cation. An explanation for this anomalous behavior is not readily evident. Interestingly, a related complex, $[Cp_2Zr(Ph)(NCMe)]BPh_4$, does not persist in the presence of excess acetonitrile, but rather undergoes insertion of NCMe into the Zr–Ph bond. The thermally stable complex thus formed, $[Cp_2Zr(NC\{Me\}Ph)(NCMe)]BPh_4$, contains but one NCMe ligand.[33] That a similar insertion process has not occurred for our W complex (**9′**) is indicated by the methylene-proton satellites ($^2J_{WH}$ = 5.9 Hz) that are observed in the ^1H NMR spectrum of **9′**.

Halide abstraction from $Cp^*M(NO)(CH_2CMe_3)Cl$ in a noncoordinating solvent such as dichloromethane does not lead to tractable products, presumably because the unsolvated 14-electron $[Cp^*M(NO)(CH_2CMe_3)]^+$, if formed, would be exceedingly reactive. The scope of ligand types that can be coordinated to the $[Cp^*M(NO)(CH_2CMe_3)]^+$ fragment remains to be ascertained. It should be noted that a family of cations isoelectronic with those in **9** and **9′** have been extensively studied by Jordan and coworkers.[34] The $[Cp'_2Zr(R)(L)]BX_4$ [R = H, Me, CH_2Ph, Ph; L = NCMe, THF; X = F, Ph] salts mediate a variety of productive insertion processes. Similar reactivity may be envisaged for complexes derived from **9** and **9′**.

Reactions of 18-Electron Derivatives of $Cp^*M(NO)(CH_2CMe_3)Cl$. In order to determine if the η^2-acyl ligands in **7** and **7′** could be displaced from their metal centers, these complexes were reacted with PMe_3. An instantaneous color change from yellow to orange occurs upon addition ot PMe_3 to complex **7′** (eq 8). The isolated product from conversion 8 for W (**10′**) is the metal-centered adduct as confirmed by its ^{31}P NMR spectrum in $CDCl_3$ in which the singlet resonance observed for the complex is flanked by W satellites (J_{PW} = 187 Hz). In addition,

---

(31) Chin, T. T.; Legzdins, P.; Trotter, J.; Yee, V. C. *Organometallics* **1992**, *11*, 913.

(32) Nakamoto, K. *Infrared and Raman Spectra of Inorganic and Coordination Compounds*, 4th ed.; Wiley-Interscience: New York, 1986; pp 280–281.

(33) Borkowsky, S. L.; Jordan, R. F.; Hinch, G. D. *Organometallics* **1991**, *10*, 1268.

(34) Jordan, R. F.; Bradley, P. K.; LaPointe, R. E.; Taylor, D. F. *New. J. Chem.* **1990**, *14*, 505 and refs therein.

Table IX. Final Atomic Coordinates (Fractional) and B_{eq} (Å^2) for (η^5,η^1-$C_5Me_4CH_2$)W(NO)(CH_2CMe_3)(PMe_3) (11′)

atom	x	y	z	B_{eq}[a]
W(1)	0.53600(2)	0.15732(2)	0.31746(3)	2.79(1)
P(1)	0.62391(15)	0.05662(12)	0.1647(3)	3.9(1)
O(1)	0.6513(4)	0.1318(4)	0.6066(7)	6.0(3)
N(1)	0.6051(4)	0.1360(3)	0.4875(7)	3.7(3)
C(1)	0.5471(6)	0.2736(4)	0.2078(9)	3.8(4)
C(2)	0.4631(7)	0.2456(4)	0.1381(8)	3.9(3)
C(3)	0.3949(6)	0.2436(4)	0.2548(9)	3.5(4)
C(4)	0.4340(5)	0.2685(4)	0.3993(9)	3.3(4)
C(5)	0.5276(6)	0.2898(4)	0.3696(9)	3.7(3)
C(6)	0.6340(6)	0.2361(5)	0.1669(13)	5.2(5)
C(7)	0.4478(7)	0.2283(6)	−0.0358(10)	6.4(5)
C(8)	0.2942(5)	0.2211(5)	0.2312(10)	5.0(4)
C(9)	0.3811(6)	0.2870(5)	0.5433(10)	4.9(4)
C(10)	0.5918(6)	0.3258(5)	0.4860(12)	5.8(5)
C(11)	0.5884(7)	0.0406(6)	−0.0358(10)	7.0(6)
C(12)	0.6294(6)	−0.0440(4)	0.2402(9)	4.9(4)
C(13)	0.7485(6)	0.0792(6)	0.150(2)	7.6(6)
C(14)	0.4306(5)	0.0595(4)	0.3364(9)	3.5(3)
C(15)	0.4010(5)	0.0212(5)	0.4893(10)	4.4(4)
C(16)	0.3758(7)	0.0828(6)	0.6119(11)	6.4(5)
C(17)	0.3123(7)	−0.0306(5)	0.4615(13)	7.5(6)
C(18)	0.4755(7)	−0.0323(5)	0.5610(10)	5.7(4)

[a] $B_{eq} = (^8/_3)\pi^2\Sigma\Sigma U_{ij}a_i^*a_j^*(a_i \cdot a_j)$

the mode of attachment of the acyl ligand has changed from η^2 to η^1. Evidence for this conclusion is two-fold. First, the carbonyl carbon resonance has shifted to higher field in the ^{13}C NMR spectrum (δ 288.00 to 264.60 ppm) of **10′** in $CDCl_3$ and shows a weak coupling to phosphorous

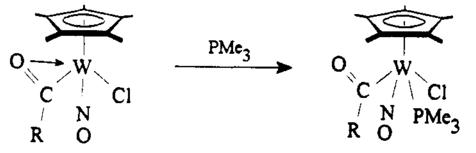

(8)

10'

(J_{CP} = 8.0 Hz) characteristic of a two-bond separation. Second, the band attributable to the carbonyl group in the mull IR spectrum of **10′** has moved to higher energy (1564 to 1634 cm^{-1}) than that in **7′**.

The reaction of Cp*Mo(NO)(η^2-C{O}CH_2CMe_3)Cl (**7**) with PMe_3 is not so straightforward. Treatment of **7** with excess PMe_3 in $CDCl_3$ forms a single organometallic product that has two different PMe_3 ligands. Since the ^1H NMR spectrum of this product reveals that the signals attributable to the methylene protons of the acyl ligand show ^{31}P coupling (28.5 and 6.9 Hz), we propose that one PMe_3 ligand is attached to the acyl carbon and one is attached to the metal, thereby causing the chloro ligand to become a counteranion. The putative salt, [Cp*Mo(NO)(C{O}{PMe_3}CH_2CMe_3)(PMe_3)]Cl, is stable only in solution in the presence of excess phosphine and decomposes readily upon removal of solvent. It should be noted that similar reactivity of acyl ligands has been demonstrated by others. Hersh has shown that treatment of CpMo(NO)(C{O}-*p*-tolyl)I with PMe_3 leads to the formation of the carbon-based phosphine adduct, CpMo(NO)(C{O}{PMe_3}-*p*-tolyl)I.[30] Similarly, Tilley has shown that the acyl carbon in Cp*Ta(C{O}$SiMe_3$)Cl_3 is prone to attack by nucleophiles such as PMe_3 and pyridine.[35]

Table X. Selected Bond Lengths (Å) and Bond Angles (deg) with ESD's in Parentheses for (η^5,η^1-$C_5Me_4CH_2$)W(NO)(CH_2CMe_3)(PMe_3) (11′)

Distances			
W(1)–P(1)	2.482(2)	C(1)–C(2)	1.42(1)
W(1)–N(1)	1.790(6)	C(1)–C(5)	1.43(1)
W(1)–C(1)	2.177(7)	C(1)–C(6)	1.44(1)
W(1)–C(2)	2.375(7)	C(2)–C(3)	1.39(1)
W(1)–C(3)	2.547(8)	C(2)–C(7)	1.52(1)
W(1)–C(4)	2.477(7)	C(3)–C(4)	1.41(1)
W(1)–C(5)	2.281(7)	C(3)–C(8)	1.51(1)
W(1)–C(6)	2.319(8)	C(4)–C(5)	1.41(1)
W(1)–C(14)	2.242(7)	C(4)–C(9)	1.47(1)
W(1)–Cp	2.048	C(5)–C(10)	1.48(1)
P(1)–C(11)	1.801(9)		
P(1)–C(12)	1.815(8)		
P(1)–C(13)	1.829(8)		
O(1)–N(1)	1.213(7)		

Angles			
P(1)–W(1)–N(1)	90.3(2)	C(1)–C(2)–C(3)	107.7(6)
P(1)–W(1)–C(6)	78.2(2)	C(1)–C(2)–C(7)	126.2(9)
P(1)–W(1)–C(14)	82.9(2)	C(3)–C(2)–C(7)	126(1)
P(1)–W(1)–Cp	136.9	C(2)–C(3)–C(4)	109.6(7)
N(1)–W(1)–C(6)	103.1(3)	C(2)–C(3)–C(8)	125.6(7)
N(1)–W(1)–C(14)	99.6(3)	C(4)–C(3)–C(8)	124.7(8)
N(1)–W(1)–Cp	124.4	C(3)–C(4)–C(5)	107.2(7)
C(6)–W(1)–C(14)	150.3(3)	C(3)–C(4)–C(9)	125.6(7)
C(6)–W(1)–Cp	70.2	C(5)–C(4)–C(9)	125.7(8)
C(14)–W(1)–Cp	111.4	C(1)–C(5)–C(4)	108.0(8)
W(1)–P(1)–C(11)	117.1(3)	C(1)–C(5)–C(10)	126.9(9)
W(1)–P(1)–C(12)	118.4(3)	C(4)–C(5)–C(10)	125.1(8)
W(1)–P(1)–C(13)	112.8(3)	W(1)–C(6)–C(1)	66.0(4)
C(11)–P(1)–C(12)	102.0(5)	W(1)–C(14)–C(15)	124.4(5)
C(11)–P(1)–C(13)	104.1(6)		
C(12)–P(1)–C(13)	100.1(4)		
W(1)–N(1)–O(1)	171.7(6)		

Dehydrohalogenation of Cp*M(NO)(CH_2CMe_3)(PMe_3)Cl (**5, 5′**) with LDA in THF gives moderate yields of the unusual dialkyl complexes **11** and **11′** in which the metallated Cp* ring serves as the second alkyl ligand (eq 9). Conversions 9 probably proceed via direct deproto-

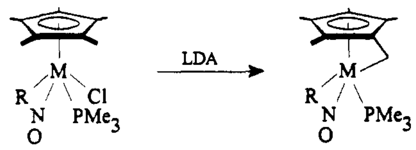

(9)

11, 11'

nation by LDA of a Me substituent of the Cp* ligand followed by intramolecular metathesis. Alternatively, deprotonation of the hydrocarbyl ligand would afford a transient alkylidene species that could rearrange to the final product. Bercaw and co-workers have established a precedent for such a rearrangement (eq 10).[36] We believe

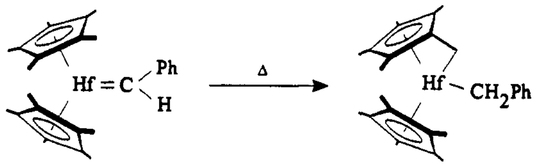

(10)

that this latter pathway is unlikely in our systems for two reasons. First, the methylene protons of **5** and **5′** are more sterically protected than the methyl groups of the Cp* ligands and LDA is a hindered base. Secondly, we have recently isolated the alkylidene complexes, CpMo(NO)(=$CHCMe_3$)L, and have shown that they are stable to at least 150 °C in C_6D_6.

---

(35) Arnold, J.; Tilley, T. D.; Rheingold, A. L.; Geib, S. J.; Arif, A. M. *J. Am. Chem. Soc.* **1989**, *111*, 149.

(36) Bulls, A. R.; Schaefer, W. P.; Serfas, M.; Bercaw, J. E. *Organometallics* **1987**, *6*, 1219.

The NMR spectra of 11 and 11′ in $CDCl_3$ exhibit four different methylene-proton resonances and four inequivalent Cp* methyl-group signals (^{1}H and APT NMR) in addition to the CMe_3 resonance for the neopentyl ligand. The two sets of methylene-proton signals show markedly different $^2J_{HH}$ couplings characteristic of their chemical environments. Thus, the neopentyl methylene protons are bound to the purely sp^3 methylene carbon and exhibit coupling constants of 12.9 Hz (Mo) and 13.8 Hz (W), whereas the methylene protons on the tucked-in Cp* ring are bound to a carbon with considerable sp^2 character and thus are only weakly coupled [2.7 Hz (Mo) and 3.6 Hz (W)]. Fortuitously, a single diastereomer of each product is isolated from reactions 9. This feature is most clearly evident by one singlet resonance in the $^{31}P\{^1H\}$ NMR spectra of both 11 and 11′ (Table III).

A single-crystal X-ray crystallographic analysis of 11′ has been performed. Its crystallographic experimental parameters are collected in Table VI, and selected intramolecular bond lengths and bond angles are summarized in Table X. An ORTEP diagram of the solid-state molecular structure of 11′ is shown in Figure 2, and this diagram clearly shows the puckering in the deprotonated Cp* ring of $(\eta^5,\eta^1\text{-}C_5Me_4CH_2)W(NO)(CH_2CMe_3)(PMe_3)$. The ring carbons, C(1)–C(5), define a plane with a mean deviation of 0.0113 Å, but the methylene carbon, C(6), is 0.8592 Å out of this plane and the angle between the Cp* plane and the plane defined by C(2), C(5), and C(6) is 23.38°. Related complexes such as $[Cp^*Ru(\eta^5,\eta^1\text{-}C_5Me_4CH_2)]BF_4$,[37] $Cp^*Hf(\eta^5,\eta^1\text{-}C_5Me_4CH_2)(CH_2Ph)$,[36] and $Cp^*Zr(\eta^5,\eta^1\text{-}C_5Me_4CH_2)(Ph)$[38] show similar interplanar angles of 14.4, 37, and 37°, respectively. Furthermore, the molecular structures of the two W complexes, $(\eta^6\text{-}C_6H_5Me)W(\eta^5,\eta^1\text{-}C_5Me_4CR_2)$ [R = Me, Ph], show 37 and 39° bending of the *exo*-methylene groups toward the W atoms.[39] Finally, it may be noted that $(\eta^5,\eta^1\text{-}C_5Me_4CH_2)W(NO)(CH_2CMe_3)(PMe_3)$ (11′) exhibits a C(1)–C(6) bond length of 1.44(1) Å which is intermediate between that expected for single and double CC bonds, thereby indicating that the deprotonated Cp* ring has some tetramethylfulvene character. For comparison, an iridium complex with a purely $\eta^4\text{-}C_5Me_4CH_2$ ligand and no iridium-methylene interaction shows a ring-methylene C–C bond length of 1.377(10) Å.[40]

Acknowledgment. We are grateful to the Natural Sciences and Engineering Research Council of Canada for support of this work in the form of grants to P.L. and a postgraduate scholarship to J.D.D. We also thank Dr. N.H. Dryden for first synthesizing $Cp^*W(NO)(CH_2CMe_3)_2$.

Supplementary Material Available: Tables of hydrogen atom coordinates, anisotropic thermal parameters, complete tables of bond lengths and bond angles, torsion angles, intermolecular contacts, and least-squares planes for complex 7 and complex 11′ and a stereoview of both crystallographically independent molecules of 7 (32 pages). Ordering information is given on any current masthead page.

OM930093B

---

[37] Kreindlin, A. Z.; Petrovskii, P. V.; Rybinskaya, M. I.; Yanovskii, A. I.; Struchkov, Yu. T. *J. Organomet. Chem.* 1987, *319*, 229.

[38] Schock, L. E.; Brock, C. P.; Marks, T. J. *Organometallics* 1987, *6*, 232.

[39] Bandy, J. A.; Mtetwa, V. S. B.; Prout, K.; Green, J. C.; Davies, C. E.; Green, M. L. H.; Hazel, N. J.; Izquierdo, A.; Martin-Polo, J. J. *J. Chem. Soc., Dalton Trans.* 1985, 2037.

[40] Glueck, D. S.; Bergman, R. G. *Organometallics* 1990, *9*, 2862.